Eur. Phys. J. C (2026) 86:808
https://doi.org/10.1140/epjc/s10052-026-15693-1

THE EUROPEAN PHYSICAL JOURNAL C

Regular Article - Experimental Physics

Search for emerging jets in pp collisions at $\sqrt{s} = 13$ TeV with the ATLAS experiment

The ATLAS Collaboration[*]

CERN, 1211 Geneva 23, Switzerland

Received: 15 October 2025 / Accepted: 11 April 2026
© CERN for the benefit of the ATLAS Collaboration 2026

Abstract A search is presented for emerging jets using 140 fb^{-1} of proton–proton collision data at $\sqrt{s} = 13$ TeV, collected by the ATLAS experiment between 2015 and 2018. The search looks for the existence of a dark sector with symmetries similar to those in quantum chromodynamics. This dark sector is populated with dark quarks, which undergo showering similar to quarks in the Standard Model, leading to a high multiplicity of long-lived dark hadrons within a dark jet. These dark hadrons subsequently decay to Standard Model particles via a new heavy scalar mediating particle ϕ. This results in jets which contain multiple displaced vertices, known as emerging jets. This analysis targets four-jet topologies, with two emerging jets and two Standard Model jets, resulting from the decay of pair-produced scalar mediators. No significant excess above the Standard Model background is observed. For dark pion proper decay lengths of 20 mm, mediator masses are excluded between 1 and 2 TeV assuming a dark pion mass of 20 GeV.

Contents

1 Introduction . . . 1
2 ATLAS detector . . . 3
3 Data and simulated events . . . 3
3.1 Signal simulation . . . 4
3.2 Background simulation . . . 4
4 Event reconstruction . . . 4
5 Event selection . . . 5
6 Machine learning classifier . . . 5
7 Background estimation . . . 6
8 Signal systematic uncertainties . . . 8
9 Results . . . 9
10 Conclusion . . . 12
A Cut-Based analysis . . . 13
References . . . 15

1 Introduction

Although there is a vast body of evidence for the existence of Dark Matter (DM) [1–3], its nature is one of the major unanswered questions in fundamental physics. Many theoretical models of particle DM have been proposed, each with corresponding interactions with the Standard Model (SM). However, after years of searching, no experiment has yet provided evidence of the particle nature of DM [4–12]. This drought of experimental confirmations has prompted the search for more exotic models of DM, including the existence of a *dark sector* (DS). The DS is an extension of the SM which contains new particles that are uncharged under the symmetries of the SM, instead having interactions governed by a new confining DS gauge group [13–15]. Although the DS and SM cannot communicate directly, interactions between DS and SM particles can be mediated by new particles that are charged under both SM and DS symmetries.

Several models propose new DS interactions which resemble quantum chromodynamics (QCD) in the SM, colloquially known as *dark QCD* [16–18]. These DS models contain quark-like particles, with N_f flavours and N_c colours, which transform under a non-Abelian gauge group SU(N_c). This new interaction is characterized by a confining scale (Λ_d) below which dark quarks (Q_d) hadronize, analogously to QCD, to form dark baryons and mesons. The lightest dark baryon could be stable, providing a DM candidate which conforms to the astrophysical evidence, while the lightest dark mesons, *dark pions* (π_d), would be unstable and decay to into SM particles via an exchange of a virtual mediator particle. Depending on the lifetimes of the dark pions, the resulting decay topology can differ greatly, giving rise to three general categories of detector signatures in collider experiments: prompt *dark jets* [19], *semi-visible jets* [20], and *emerging jets* (EJs) [21]. In each case there is some component of the DS which is unstable, and therefore decays back to the SM, and so dark QCD signatures are characterized by a double shower and hadronization, once in the DS and once in the SM which gives rise to wider jets with higher charged-track

[*] e-mail: atlas.publications@cern.ch

Published online: 14 July 2026

multiplicities. For the case of dark jets, where all the dark hadrons decay promptly back to SM particles, these features allow them to be differentiated from SM hadronic jets. In the case of semi-visible jets, however, some of the dark hadrons decay promptly, while others are stable, and therefore carry missing transverse energy ($E_{\mathrm{T}}^{\mathrm{miss}}$) which goes undetected; this results in $E_{\mathrm{T}}^{\mathrm{miss}}$ aligned with the hadronic jet which can be used to distinguish semi-visible jets from SM jets. Finally, in the case of EJs, all of the dark hadrons are unstable, but are also long-lived, and therefore they decay within the detector volume but displaced from the initial collision, giving rise to multiple displaced vertices (DVs) contained in the jet cone. Due to the exponential distribution of the π_d decay times, these DVs occur at varying radial distances, giving rise to the emerging quality of the EJ.

Using the proton–proton (pp) collisions of the LHC, both ATLAS and CMS collaborations have carried out dedicated searches for different dark-QCD scenarios, characterized by various production modes and decay topologies. Both ATLAS and CMS have searched for semi-visible jets in Run 2 data [22–24]. ATLAS has set limits on a search for promptly decaying dark hadrons from the resonant production of dark jets [25]. In Run 1, ATLAS performed a search for hadronic decays of long-lived particles which give a displaced jet signature [26]. In Run 2, CMS performed two searches specifically targeting EJ signatures by looking for pair-produced, *bifundamental*,[1] scalar mediators (ϕ) resulting in a four-jet topology [27,28]. In Run 3 ATLAS produced a search for EJs that focused on the resonant production of a vector mediator (Z') resulting in a two-jet topology [29]. The Run 3 analysis also included an interpretation using $t-$channel production of the bifundamental scalar mediator with two, three, or four jets in the final state, which causes the production cross-section to be dependent on the Yukawa coupling of the mediator. For dark pions with proper decay length of 10 mm and mass of 10 GeV, the CMS search produced limits which excluded scalar mediator masses up to 1.95 TeV, and the ATLAS search produced limits which excluded vector mediator masses up to 2.55 TeV.

This search looks for pair-produced dark scalar mediators in pp collisions at $\sqrt{s} = 13$ TeV. The two production modes considered are $q\overline{q}$ annihilation (shown in Fig. 1) and gluon–gluon fusion. These production modes are expected to dominate over $t-$channel production used in the Run 3 search [21]. Both modes proceed via a virtual gluon which produces a pair of dark mediators ($\phi^\dagger\phi$). Each dark mediator immediately decays into a dark quark and a SM quark, both of which hadronize in their corresponding sectors, resulting in a SM jet and an EJ. The final topology is a four jet final state, with two emerging jets and two SM jets. The Yukawa coupling (κ) is assumed to be sufficiently small, that diagrams proportional to κ^4 are ignored.

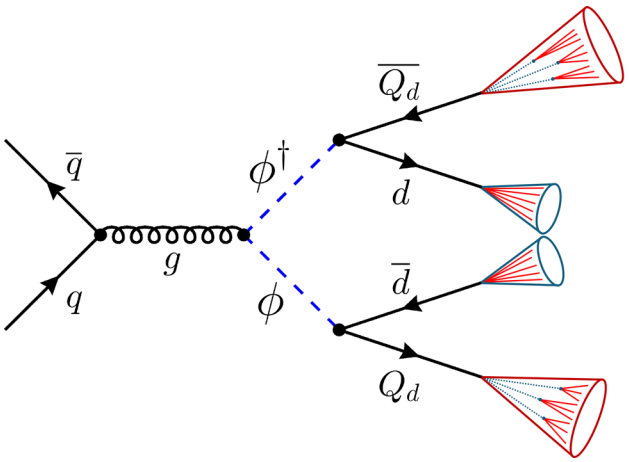

Fig. 1 Feynman diagram of the pair-production of dark scalar mediators, ϕ, via quark–antiquark annihilation. The resulting four jets are shown as cones for illustrative purposes. Dashed lines within the cones represent the trajectories of dark pions, solid lines within the cones represent the trajectories of SM particles

An *unflavoured* model (similar to the most-minimal model in Ref. [30]) is considered, where the Yukawa coupling between the dark mediator and the SM quark is only non-zero for SM down quarks,[2] giving only light SM jets in the final state. The choice of ϕ coupling only to SM down quarks or SM up quarks is arbitrary in the unflavoured model, as both will give only light SM jets in the final state; the down-type coupling is chosen following Ref. [21]. The Run 3 search considered a *flavour-aligned* model of the bifundamental scalar, where the scalar mediator can couple to any down-type standard model quark. This allows for heavy-flavour jets in the final state when kinematically allowed.

A two-stage machine learning (ML) based classifier is used to separate EJ-like events from the dominant QCD multijet background. The contribution from this background is estimated using a data-driven approach based on the ABCD method. Other background processes, such as top quark pair-production, were considered, but their contributions are suppressed to a negligible level by analysis preselections.

The paper is structured in the following way: Sect. 2 gives a description of the Run 2 configuration of the ATLAS detector, while Sect. 3 gives an overview of the collected dataset, and the simulated samples produced for this analysis. Sections 4 and 5 detail how the various physics objects are reconstructed, and how events are selected for the analysis. The ML classifier is described in Sect. 6. Then, Sect. 7 outlines

[1] Bifundamental means that it is charged under both the symmetries of Dark QCD and Standard Model QCD as $SU(3)_{QCD} = 3$ and $SU(N_c)_{Dark} = N_c$. Note that the bifundamental scalar is labeled X_d in Ref. [21] and X_{dark} in Ref. [27,28].

[2] In addition to $SU(3)_{QCD} = 3$ charge, the mediator has SM $U(1) = \frac{1}{3}$ charge, since it couples to down quarks.

the background estimation method and Sect. 8 documents the systematic uncertainties. Finally, the results of the analysis are presented in Sect. 9 with conclusions given in Sect. 10.

2 ATLAS detector

The ATLAS detector [31] at the LHC covers nearly the entire solid angle around the collision point.[3] It consists of an inner tracking detector surrounded by a thin superconducting solenoid, electromagnetic and hadronic calorimeters, and a muon spectrometer incorporating three large superconducting air-core toroidal magnets.

The inner-detector system (ID) is immersed in a 2 T axial magnetic field and provides charged-particle tracking in the range $|\eta| < 2.5$. The high-granularity silicon pixel detector covers the vertex region and typically provides four measurements per track, the first hit generally being in the insertable B-layer (IBL) installed before Run 2 [32,33]. It is followed by the SemiConductor Tracker (SCT), which usually provides eight measurements per track. These silicon detectors are complemented by the transition radiation tracker (TRT), which enables radially extended track reconstruction up to $|\eta| = 2.0$. The TRT also provides electron identification information based on the fraction of hits (typically 30 in total) above a higher energy-deposit threshold corresponding to transition radiation.

The calorimeter system covers the pseudorapidity range $|\eta| < 4.9$. Within the region $|\eta| < 3.2$, electromagnetic calorimetry is provided by barrel and endcap high-granularity lead/liquid-argon (LAr) calorimeters, with an additional thin LAr presampler covering $|\eta| < 1.8$ to correct for energy loss in material upstream of the calorimeters. Hadronic calorimetry is provided by the steel/scintillator-tile calorimeter, segmented into three barrel structures within $|\eta| < 1.7$, and two copper/LAr hadronic endcap calorimeters. The solid angle coverage is completed with forward copper/LAr and tungsten/LAr calorimeter modules optimised for electromagnetic and hadronic energy measurements, respectively.

The muon spectrometer (MS) comprises separate trigger and high-precision tracking chambers measuring the deflection of muons in a magnetic field generated by the superconducting air-core toroidal magnets. The field integral of the toroids ranges between 2.0 and 6.0 T m across most of the detector. Three layers of precision chambers, each consisting of layers of monitored drift tubes, cover the region $|\eta| < 2.7$, complemented by cathode-strip chambers in the forward region, where the background is highest. The muon trigger system covers the range $|\eta| < 2.4$ with resistive-plate chambers in the barrel, and thin-gap chambers in the endcap regions.

The luminosity is measured mainly by the LUCID–2 [34] detector that records Cherenkov light produced in the quartz windows of photomultipliers located close to the beampipe.

Events were selected by the first-level trigger system implemented in custom hardware, followed by selections made by algorithms implemented in software in the high-level trigger [35]. The first-level trigger accepted events from the 40 MHz bunch crossings at a rate close to 100 kHz, which the high-level trigger further reduced in order to record complete events to disk at about 1.25 kHz.

A software suite [36] is used in data simulation, in the reconstruction and analysis of real and simulated data, in detector operations, and in the trigger and data acquisition systems of the experiment.

3 Data and simulated events

This analysis uses 140 fb^{-1} of pp collision data collected at $\sqrt{s} = 13$ TeV by the ATLAS experiment between the years of 2015 and 2018, corresponding to Run 2 of the LHC. The dataset contains only those events recorded during stable beam conditions, with all detector subsystems operating properly. Standard data-quality requirements are used to ensure reliable reconstruction of the physics objects [37].

Monte Carlo (MC) simulation events, generated with Pythia 8.230 [38], are used to optimise the analysis strategy, evaluate the signal efficiency, and test the background estimation methods. Matrix element generation of the hard scattering process and subsequent showering uses the NNPDF2.3lo [39] parton distribution function (PDF) set, with the A14 set of tuned parameters [40]. Pile-up, the effect of multiple interactions in the same and neighbouring bunch crossings, is modelled by combining the results of the simulated hard-scattering event with simulated inelastic pp events generated with Pythia 8.186 [41] and the A3 set of tuned parameters [42]. The interaction of the collision products with the ATLAS detector, and subsequent detector response [36], are modelled by passing MC events through a detailed map of the detector material implemented into Geant4 [43]. MC events then are reconstructed using the same algorithms applied to the data.

[3] ATLAS uses a right-handed coordinate system with its origin at the nominal interaction point (IP) in the centre of the detector and the z-axis along the beam pipe. The x-axis points from the IP to the centre of the LHC ring, and the y-axis points upwards. Polar coordinates (r, ϕ) are used in the transverse plane, ϕ being the azimuthal angle around the z-axis. The pseudorapidity is defined in terms of the polar angle θ as $\eta = -\ln\tan(\theta/2)$ and is equal to the rapidity $y = \frac{1}{2}\ln\left(\frac{E+p_z}{E-p_z}\right)$ in the relativistic limit. Angular distance is measured in units of $\Delta R \equiv \sqrt{(\Delta y)^2 + (\Delta\phi)^2}$.

3.1 Signal simulation

Samples of $pp \to \phi^\dagger\phi \to \overline{Q}_d q Q_d \overline{q}$ are produced at leading-order (LO) using the Hidden Valley [44] implementation in PYTHIA 8.230, which handles the showering and hadronization of the dark quarks within the DS. Mediator masses ranging from 1 TeV to 2.2 TeV are used, with the corresponding pair-production cross-sections estimated using calculations from Supersymmetry, where stop–antistop pairs are used as a proxy for the dark mediators. The cross-sections are calculated at approximate next-to-next leading-order and next-to-next leading-logarithm (NNLOapprox + NNLL) using NNLL- FAST [45,46]. Cross-section values are multiplied by a factor of N_c, for the $N_c = 3$ model this gives values in the range from 20.5 fb at $M_\phi = 1$ TeV to 0.015 fb at $M_\phi = 2.2$ TeV. Theoretical uncertainties corresponding to parton distribution functions, QCD scale, and resummation of Coulomb corrections are also produced using NNLL-FAST for each mediator mass.

Benchmark signal models are produced with $N_c = 3$, $N_f = 7$, following Ref. [21] to ensure a QCD-like DS. For a given N_c, there are a range of values for N_f, such that the running of the dark strong coupling (α_d) is still asymptotically free, $N_f = 7$ is the centre of that range.

The dark confinement scale is used to set the masses of the DS particles with the following scheme: $\Lambda_d = m_{Q_d} = 2\, m_{\pi_d} = \frac{m_{\rho_d}}{2}$. This forces the heavier dark mesons such as the dark rho to decay into dark pions ($\rho_d \to \pi_d\pi_d$), which occurs within the DS and therefore proceeds quickly. The subsequent dark pion decay to SM down quarks ($\pi_d \to d\bar{d}$) proceeds via t-channel exchange of a dark mediator. The decay is slow due to the large mass difference between the ϕ and π_d, giving rise to the macroscopic lifetimes of the dark pions. The production of dark baryons, which are suppressed by a factor of $1/N_c^2$ [20], or dark mesons other than the ρ_d and π_d, is not considered.

Three choices of Λ_d are used, corresponding to m_{π_d} values of 5, 10, and 20 GeV. These values ensure that the decay of the dark pion into jets is valid, since lower mass π_d would decay to distinct hadronic final states [47,48]. For dark pion masses much larger than $\mathcal{O}(10)$ GeV, the reduced phase space for dark pion production leads to a more diffuse spray of few dark pions giving a displaced jet signature, while this analysis targets the emerging jets signature with a collimated spray of many dark pions.

The dark pion lifetime ($c\tau_{\pi_d}$), as a function of the other phenomenological parameters of the model, is given by [21]:

$$c\tau = \frac{80\text{ mm}}{\kappa^4}\left(\frac{2\text{ GeV}}{f_{\pi_d}}\right)^2\left(\frac{100\text{ MeV}}{m_q^{\text{SM}}}\right)^2\left(\frac{2\text{ GeV}}{m_{\pi_d}}\right)\left(\frac{M_\phi}{1\text{ TeV}}\right)^4 \quad (1)$$

Table 1 Signal model parameters used to give the model grid for the analysis

M_ϕ [TeV]	1.0, 1.4, 1.6, 1.8, 2.0, 2.2
m_{π_d} [GeV]	5, 10, 20
$c\tau_{\pi_d}$ [mm]	1, 2, 5, 20, 75, 150, 300, 500, 1000

where κ is the Yukawa coupling between the dark mediator and the quarks, f_{π_d} is the dark pion decay constant (analogous to the pion decay constant in the SM), and m_q^{SM} is the mass of the SM quark which the mediator couples to (in this case the SM down quark). A consistent set of dark pion lifetimes can be set for each choice of M_ϕ or m_{π_d} by varying the Yukawa coupling. Samples are produced for proper decay lengths between 1 mm and 1000 mm, such that the majority of the dark pions decay within the tracking detectors. Table 1 gives a summary of the model parameters used in the signal MC samples for this analysis.

3.2 Background simulation

While the background estimation strategy described in Sect. 7 is fully data-driven, background MC samples are produced to optimise the analysis methodology.

The multijet QCD background [49] was generated using PYTHIA 8.230 with dijet production matrix elements calculated at LO. The NNPDF2.3LO PDF set is used for matrix element generation, showering, and multi-parton interactions, with the A14 set of parameters.

Samples of $t\bar{t}$ events were used to determine their contribution to the background. These were produced at next-to-leading-order (NLO) with POWHEG BOX V2 [50–52] using $h_{\text{damp}} = 1.5\, m_t$ [53], then interfaced with PYTHIA 8.230 for parton showering and hadronization. The decays of hadrons containing b and c quarks common in $t\bar{t}$ decays are performed by EVTGEN 1.6.0 [54]. The contribution of $t\bar{t}$ events was less than 0.1% in the search region after the analysis selections (described in Sect. 5), and therefore are not considered in the background estimate.

4 Event reconstruction

The standard ATLAS track reconstruction in Run 2 uses a combinatorial Kalman filter [55] to create tracks from energy deposits in the ID. It is optimised for reconstructing tracks from prompt charged particles with $p_{\text{T}} > 500$ MeV and transverse impact parameters (d_0) less than 10 mm, but is largely insensitive to tracks which are displaced from the interaction point (IP) as a result of the decay of neutral long-lived particles. In order to increase the tracking acceptance to displaced signatures, a secondary reconstruction for large

impact parameter tracks is performed on hits in the ID not associated with tracks from the standard track reconstruction. This dedicated Large Radius Tracking (LRT) [56] greatly relaxes the impact parameter selection to $|d_0| < 300$ mm, with a stricter momentum requirement of $p_{\mathrm{T}} > 900$ MeV.

Events are required to have a primary vertex, associated to the hard scatter interaction, which must have at least two tracks associated with it [57]. Because there may be several interaction vertices within the event, the primary interaction vertex is selected as the one with the largest $\sum p_{\mathrm{T}}^2$ of all associated standard tracks.

Secondary displaced vertices (DVs) are reconstructed using a dedicated algorithm seeded with tracks from both the standard and LRT track collections [58]. In order to mitigate the contribution of background DVs from SM processes, material interactions, and fakes, a series of analysis-specific requirements were defined which apply successive selections to the DVs. These aim to reject background DVs while maintaining high efficiency of selecting signal DVs. The first selections are on the radial and longitudinal position of the DV, restricting DVs to where the LRT tracking is efficient, $r_{\mathrm{DV}} < 300$ mm and $|z_{\mathrm{DV}}| < 300$ mm. Next, to reduce the contribution from long-lived neutral kaons (K_S^0), the DVs are required to have $m_{\mathrm{DV}} > 0.7$ GeV, where the mass is computed as the invariant mass of the sum of the four-momenta of all tracks associated to the DV, where each track is assumed to be from a SM charged pion. The effect of random track crossings being reconstructed as DVs is limited by applying requirements on the minimum of the impact parameters of all tracks matched to the DV ($\min |d_0| < 10$ mm, $\min |z_0| < 100$ mm), and the transverse momenta ($p_{\mathrm{T}}^{\mathrm{DV}} > 2.5$ GeV) of the reconstructed DVs. Selections on the associated uncertainties of the impact parameters ($\sigma_{d_0} < 0.25$ mm, $\sigma_{z_0} < 2.25$ mm) help to remove DVs reconstructed from LRT fakes. Finally, a map of the ID material obtained with Run 2 data [59] is used to veto DVs which are located in regions of known detector material.

Jets are reconstructed using energy deposits in the calorimeters. Topological clusters [60,61] are reconstructed into jets using the anti-k_t algorithm using a distance parameter of $R = 0.4$, and are calibrated at the electromagnetic scale. In order to be counted in the jet collection, jets are required to have $p_{\mathrm{T}} > 50$ GeV and $|\eta| < 2.7$.

Additionally, jets containing b-hadrons (b-jets) are tagged using the DL1r algorithm [62], passing the 85% efficiency working point, and are used to estimate the contribution of heavy-flavour within the multijet QCD background. In order to keep jets with associated displaced tracks, which are expected with the emerging jets topology, no attempt is made to match jets to the primary vertex.

5 Event selection

Events are selected using an unprescaled trigger which requires at least 4 jets with a p_{T} threshold of 120 GeV [63]. The trigger has a Level 1 requirement of three jets that each deposit at least 50 GeV of transverse energy, within a region of 0.8×0.8 in $\eta - \phi$ space [64,65] in the calorimeters. As described above, the analysis uses a set of reconstruction techniques which were non-standard and computationally expensive in Run 2. Thus, this special reconstruction was only run on events which passed the baseline topology requirements of at least four jets, each with transverse momentum $p_{\mathrm{T}} > 120$ GeV and $|\eta| < 2.4$. Events matching this topology are selected using jets before calibration, which is applied after reconstruction.

A dedicated emerging jets trigger was implemented in Run 3, which allowed for the analysis in Ref. [29] to increase their sensitivities to lower jet multiplicity topologies. However, in Run 2, only the 4-jet trigger provided sufficient background rejection to allow for sensitivity to the emerging jets models.

Requirements are imposed on the four highest p_{T} jets within the event to ensure an emerging jet-like topology. The scalar sum p_{T} of these jets (H_{T}) is required to be greater than 1 TeV. At least one of the four highest p_{T} jets is also required to have a well-defined prompt track fraction (PTF):

$$\mathrm{PTF} = \frac{1}{p_{\mathrm{T}}^{\mathrm{Jet}}} \sum_{i \in \mathrm{tracks}} \left(p_{\mathrm{T},i} \left| \frac{|d_{0,i}|}{\sigma_{d_0,i}} < 3 \right. \right). \tag{2}$$

For jets within $|\eta| < 2$, the PTF is computed if at least one standard track with $p_{\mathrm{T}}^{\mathrm{Track}} \geq 2$ GeV can be matched within $\Delta R < 0.4$, even if it does not meet the promptness criterion of the d_0 significance.

Finally, events are required to have at least one displaced vertex, passing all the selections defined above, which is matched to a reconstructed jet, to ensure the event meets the key criterion of emerging jets. This jet-matching for DVs is done using a loosened angular distance criterion of $\Delta R < 0.6$ between the DV position and the jet axis. This looser selection is used to account for the potential of jet-splitting within the EJs, where certain combinations of model parameters result in more diffuse sprays of high energy dark pions, which can potentially be reconstructed as individual jets, rather than a single emerging jet. This effect both inflates the jet multiplicity (N_{Jet}) of the event and decreases the displaced vertex multiplicity of the reconstructed jets.

6 Machine learning classifier

The analysis uses a two-stage ML approach using boosted decision trees (BDTs) implemented with the Toolkit for Mul-

Table 2 List of variables used in training for the jet-level boosted decision tree

Observable	Description
E_{Jet}	Jet energy, measured directly from calorimeter deposits
$m_{\text{Jet}} = \sqrt{\left(\sum_i E_i\right)^2 - \left(\sum_i \vec{p}_i\right)^2}$	Jet mass, invariant mass from the sum of topological clusters
$W_{\text{Jet}} = \frac{1}{p_{\text{T}}^{\text{Jet}}} \sum_i p_{\text{T},i} \Delta R_i$	Jet width, p_{T}-weighted angular spread of topological clusters
η_{Jet}	Jet pseudorapidity

Table 3 List of variables used in training for the event-level boosted decision tree

Observable	Description
R_{Jet}^{1-4}	BDT response of the four highest p_{T} jets, individually
$H_{\text{T}} = \sum_{j=1}^{4} p_{\text{T},j}$	Scalar sum of the four highest p_{T} jet transverse momenta
minPTF	The minimum PTF value in the four highest p_{T} jets
N_{Jet}	Reconstructed jet multiplicity
S_{T}	Transverse sphericity

tivariate Analysis (TMVA) [66]. The first step trains a BDT on jet-level information to select EJ candidates, while the second step uses a BDT trained on event-level information, including the BDT scores of the four highest p_{T} jets, to separate EJ signal events from SM multijet background. A cut-based version of the analysis, which is not optimized to the same degree as the ML strategy, is described in Appendix A and included in HEPData to aid with reinterpretation of the results.

In order to avoid biasing the results, both signal and background events which pass the selections defined in Sect. 5 are separated into two equal sets. The first set is used only for training both stages of the BDT and the second is used for testing. While the two sets are statistically independent, their BDT response distributions are consistent within the MC statistical uncertainties, showing the classifier is not overtrained. Both the jet- and event-level BDTs are trained on all of the signal MC samples mixed together, with background events sampled equally from across the full p_{T} spectrum of the multijet MC. The full training set comprises over 9 million events.

The jet-level BDT is trained on each of the four highest p_{T} jets in the event, using the jet-level observables given in Table 2. After training, the individual jet-level BDT responses (R_{Jet}) of the four highest p_{T} jets are used as inputs to the event-level BDT.

In addition to the four highest p_{T} jet BDT responses, the event-level BDT takes several observables which are used to help separate signal and background. The full list is summarized in Table 3. One of the observables, transverse sphericity (S_{T}), is an isotropy measure [67], which characterizes the shape of the event. Background events, for which the majority of the event activity is concentrated in the two highest p_{T} jets (often balanced in the transverse plane), are expected to have values of S_{T} close to 0. On the other hand, signal events tend to have a larger multiplicity of jets arranged more isotropically, leading to transverse sphericity values closer to 1.

Figure 2 shows the event-level BDT response observable (R) evaluated on background MC and a selection of signal models. In general, models which present as less SM-like are better separated from multijet background. For this reason, higher M_ϕ models tend to higher BDT responses, but the sensitivity becomes limited by the reduced cross-sections. With respect to the dark pion lifetime, only models with very small $c\tau_{\pi_d}$ are difficult to separate from the background, however sensitivity is also lost for very long lifetimes since more of the π_d decay outside of the tracker acceptance to reconstruct a displaced vertex, so the higher BDT responses are seen in intermediate lifetime models. The BDT is largely insensitive to m_{π_d}, with the 10 and 20 GeV models being only slightly better separated than the 5 GeV models.

An additional selection of $R > -0.2$ is applied to improve the background estimation discussed in Sect. 7. This requirement removes mainly background events, with at most 0.1% impact on the signal efficiency.

7 Background estimation

The dominant background for this analysis is QCD multijet production. However, these processes are difficult to properly model in simulation, thus the background estimate is produced using a data driven technique modified from the ABCD method.

The ABCD method employs a 2D parameter space divided into four regions (labelled A, B, C, and D) by applying selection criteria on each of the two variables. If the background distributions of these variables are independent, the ratios of expected background yields are related by: $\frac{N_A}{N_B} = \frac{N_C}{N_D}$. If the

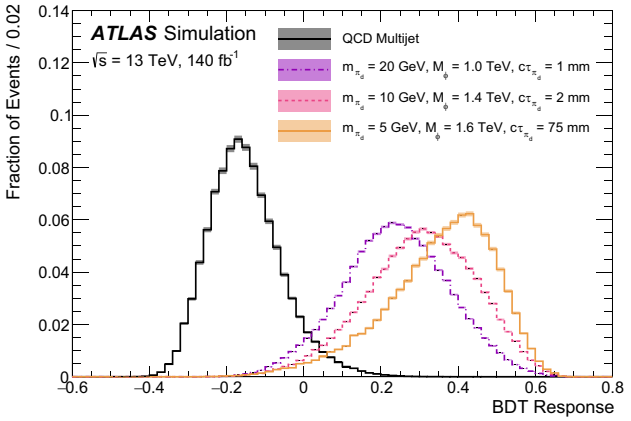

Fig. 2 Normalized event-level BDT response distribution for the QCD multijet background, with three selected signal samples for comparison

plane is designed such that the background primarily populates regions B, C, and D (labelled control regions, CRs), while the signal is concentrated in region A (labelled signal region, SR), the background yield in the SR can be estimated as:

$$N_A = N_B \times \frac{N_C}{N_D} \tag{3}$$

When performing the final statistical analysis, any signal contamination in the CRs is accounted for using a simultaneous fit, as described in Sect. 9.

The ABCD plane is defined using the event-level BDT response and the number of jet-matched displaced vertices in the event (N_{DV}). The distributions of events in the ABCD plane are shown for data and an example signal model in Fig. 3. The SR is defined by $R \geq 0.2$ and $N_{\text{DV}} \geq 2$. Control regions B and C are defined by inverting one of the two selections, and region D is defined by inverting both selections. For signal models with $M_\phi = 1.6$ TeV and $m_{\pi_d} = 10$ GeV, the full set of SR selections have efficiencies which vary between 1.4% for $c\tau_{\pi_d} = 1000$ mm and 72% for $c\tau_{\pi_d} = 20$ mm.

To account for non-negligible correlations between the two variables, CRs C and D are subdivided and the ratio $\frac{N_C}{N_D}$ is calculated in each subdivision. This is then fit with a two-parameter linear function which can be extrapolated into the SR. This function then replaces the ratio in Eq. 3, to become:

$$N_A = (p_0 \cdot R_B + p_1) \times N_B \tag{4}$$

where p_0 and p_1 are the slope and y-intercept of the linear function, respectively, and R_B is the event-weighted mean BDT response value within region B. The statistical uncertainty on the background estimation is a combination of the propagated statistical uncertainties from the fit parameters and the statistical uncertainty from the counts in region B. This corresponds to an uncertainty of 5% on the final background estimate.

In order to validate the background estimation method, two validation regions (VRs) are constructed. The Low-H_{T} VR is defined by inverting the H_{T} requirement used in the event selection to be $H_{\text{T}} < 1$ TeV, while keeping the other selections in place. This allowed for the construction of another ABCD plane using a background enriched region where data could be analysed without biasing the method. The Low-H_{T} VR is further restricted to be between 775 GeV $\leq H_{\text{T}} <$ 1000 GeV to ensure good modelling, which rapidly deteriorates at lower H_{T} values. Since the H_{T} requirement is inverted, signal contamination in the Low-H_{T} VR is below 0.001% for all signal models.

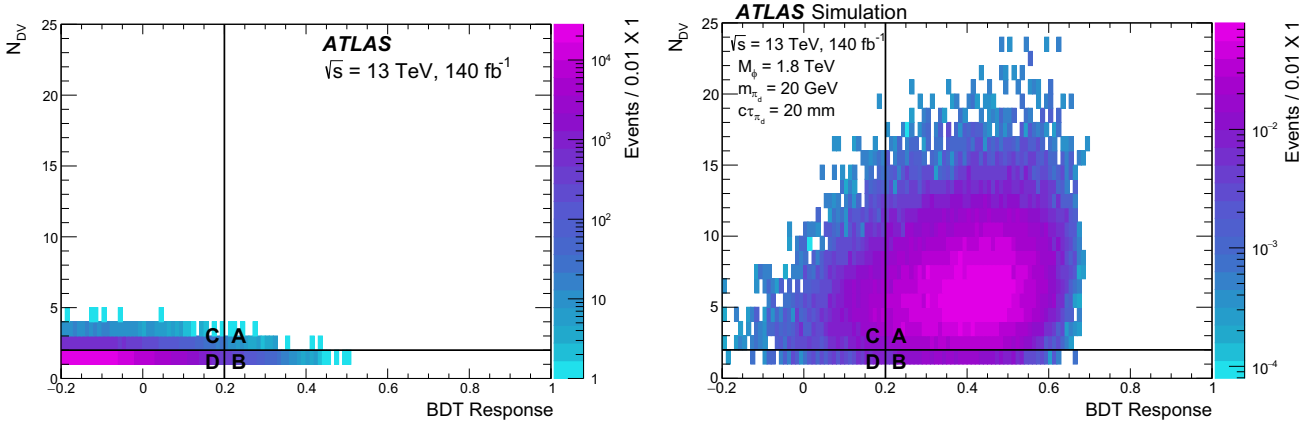

Fig. 3 Distributions of events in the ABCD plane for (left) Run 2 data and (right) an example signal model with parameters: $m_{\pi_d} = 20$ GeV, $M_\phi = 1.8$ TeV, and $c\tau_{\pi_d} = 20$ mm. The signal events are scaled to the pair-production cross-section for $pp \to \phi^\dagger\phi$ at $M_\phi = 1.8$ TeV, and normalized to the integrated luminosity of the dataset

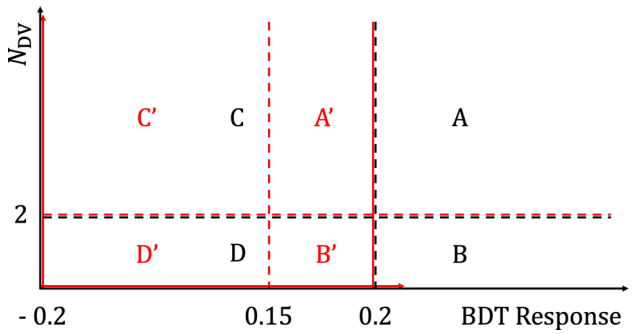

Fig. 4 Schematic diagram of the Shifted-ABCD VR constructed in CRs C and D. The four new regions are shown in red, and labeled A', B', C', and D'. The actual ABCD plane regions are shown in black for comparison

Table 4 Predicted and observed counts in the A' regions of the Low-H_T VR and the Shifted-ABCD VR, using the modified ABCD method. Quoted uncertainties are statistical only

Region	Low-H_T VR	Shifted-ABCD VR
Predicted Counts	25 ± 3	215 ± 8
Observed Counts	24	209

The second VR is constructed using CRs C and D from the ABCD plane, which have the largest contribution of background events, and the smallest signal contamination. The Shifted-ABCD VR, shown in Fig. 4, is defined with an additional selection on the BDT response, along with the same selection on N_{DV} used in the actual ABCD plane, to define four new regions. The pseudo-signal region A' is defined for $0.15 \leq R < 0.2$ and $N_{DV} \geq 2$, with the corresponding primed CRs defined by inverting one or both of the selections. Since it is much closer to the actual SR, signal contamination is slightly higher in region A' than in the Low-H_T VR, however, all models still contribute less than 10% of the total MC event yield.

The predicted and observed counts in the SRs of both the Low-H_T VR and the Shifted-ABCD VR are given in Table 4. The modified ABCD method is shown to predict background contributions which agree with the observed yields within their respective uncertainties. The per-bin closure in both validation regions was also measured to be within 1σ for all bins.

The relative difference of 3% between the predicted and observed background yields in region A' of the Shifted-ABCD VR is used as a systematic uncertainty for potential non-closure of the modifed ABCD method in the actual SR. Both the statistical uncertainty and the systematic uncertainty on the background estimation method are included separately in the statistical analysis (discussed in Sect. 9).

The closure of the modified ABCD method was also tested using QCD multijet simulation. Good agreement of the predicted and observed event yields in the SR was found, with per-bin closure within 2σ for all bins in the signal region. This closure held both inclusively, and when tested on heavy-flavour QCD production by selecting events where at least one of the four highest p_T jets is b-tagged using either the DL1r classifier or truth-level information.

8 Signal systematic uncertainties

Experimental uncertainties relating to instrumentation or reconstruction are assigned to the modelling of simulated signal samples. These systematic uncertainties include contributions from jets, tracks and displaced vertices, luminosity, as well as a dedicated uncertainty for the prompt track fraction.

The systematic associated with jets has contributions from the jet energy scale (JES), jet energy resolution (JER) [68], and jet mass scale (JMS) [69]. Jets are varied within the uncertainties for each of these contributions and the effects are propagated to the final signal yield. The resulting uncertainty depends primarily on the mediator mass of the signal sample, with dark pion lifetime having a larger effect at smaller mediator masses. The combined systematic varies between 1% for $M_\phi = 2.2$ TeV and 13% for $M_\phi = 1$ TeV.

Uncertainties from tracks and displaced vertices are derived from a combination of sources to account for both the standard and large-radius tracks. The uncertainty from LRT is derived from comparisons of events consistent with $K^0_S \rightarrow \pi^+\pi^-$ between simulation and data, and follows a prescription defined in Ref. [70]. To assess the impact, the track collection is varied according to these differences, summed in quadrature with the 1.7% systematic uncertainty associated with standard tracking [71], and then vertex reconstruction is repeated using the altered set of tracks. These changes are eventually propagated to track and DV observables, in particular N_{DV}, which gives the dominant source of uncertainty. In this case, the dark pion lifetime has the biggest impact on the size of the uncertainty, which varies between 0.5% for $c\tau_{\pi_d} = 2$ mm and 39% for $c\tau_{\pi_d} = 1000$ mm. The mediator mass also has an impact on the systematic uncertainty, since lower M_ϕ result in lower multiplicities of dark pions.

The dedicated systematic uncertainty to cover the modelling of PTF is determined by comparing the distribution of minPTF in data and background MC using the Low-H_T VR region. Per-event weights are created based on the differences, which are then used to reweight the signal samples. The final uncertainty is taken as the difference in the signal yield and varies between 1% and 12%, where the combination of lower M_ϕ and $c\tau_{\pi_d}$ result in larger uncertainties.

Pile-up conditions during different data-taking periods are modelled by reweighting simulated events, such that the aver-

Table 5 Predicted number of background events, including statistical and systematic uncertainties, and observed event yield in the SR

Event Yield in the SR	
Prediction	112 ± 6 (stat.) ± 4 (syst.)
Observed yield	103

age number of interactions per bunch crossing matches the observed distribution in data. These contributions depend on the inelastic pp cross-section, so the difference between predicted and measured values [72] are propagated as a systematic variation to reweighted events. The pile-up uncertainty varies between 0.3% for $M_\phi = 1$ TeV and 5% for $M_\phi = 2$ TeV.

Signal MC events are scaled to the integrated luminosity of the dataset, and are therefore subject to the uncertainty associated with the measurement of the total luminosity. For the full Run 2 dataset, the uncertainty is 0.8% [73], obtained using the LUCID-2 detector [34].

Theoretical uncertainties relating to the production of the dark mediators are applied to the theoretical cross-sections used for limit-setting in Sect. 9. These uncertainties are produced using NNLL- FAST [45,46] along with the corresponding cross-sections, and are roughly proportional to the mediator mass. Values range from 11% at $M_\phi = 1$ TeV to 27% for $M_\phi = 2$ TeV.

The dominant source of uncertainty varies between the different signal models, but in most cases the tracking and vertexing systematic is the leading contribution.

9 Results

The predicted background yield in the SR, determined from the extrapolated fit of the modified ABCD method (described in Sect. 7), and corresponding observed yield is given in Table 5. No excess above the data-driven background estimate is observed.

In the absence of excess data events, a hypothesis test is performed using a simultaneous likelihood fit which incorporates the methodology of the modified ABCD method, and accounts for any signal leakage into the CRs. Signal and background systematic uncertainties are included in the fit as Gaussian nuisance parameters.

The likelihood fit is constructed with the product of Poisson probabilities of observing the event yield in each region $i \in \{A, B, C, D\}$ of the ABCD plane, subdivided into j bins across the BDT response ($N^{\text{Obs}}_{i,j}$) in order to perform the linear fit across regions C and D, which is then extrapolated into the regions A and B. The CRs C and D are divided into 8 bins across the BDT response, while the SR and CR B are divided into 4–5 bins, where the number of bins is adjusted to ensure there are sufficient data events in each bin of region

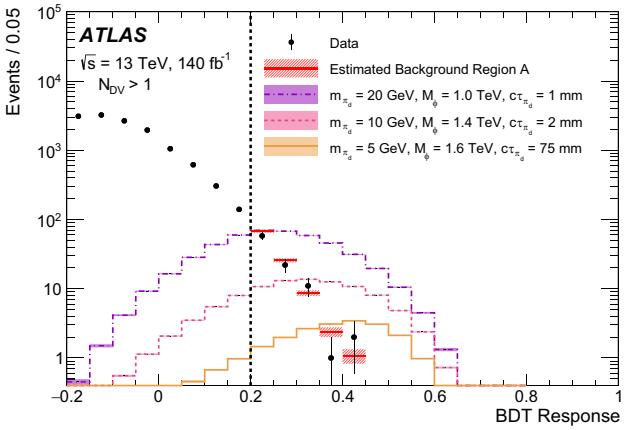

Fig. 5 Comparison of the data with $N_{\text{DV}} > 1$ and the estimated background in the SR using the modified ABCD method. The division between the SR and CR is shown by the vertical dashed line. In the final fit, the bins with $R > 0.4$ are combined into a single bin. Three selected signal samples are included for comparison

B. The expected number of events in a given bin of region A ($N^{\text{Exp}}_{A,j}$) is then given by:

$$N^{\text{Exp}}_{A,j} = (p_0 \cdot R_j + p_1) \times N^{\text{Exp}}_{B,j} + \mu \cdot N^{\text{Sig}}_{A,j} \tag{5}$$

where p_0 and p_1 are again the slope and y-intercept, respectively, of the linear fit extracted from the subdivided regions C and D. R_j is the event weighted mean value of the BDT response within the j bin of region B. The signal strength parameter, μ, is fit simultaneously across the entire ABCD plane, and $N^{\text{Sig}}_{A,j}$ is the expected signal contribution in each bin of A, taken from signal MC. The agreement between the extrapolated background estimate, as determined by the likelihood fit, and the observed data in the SR is shown in Fig. 5. Only data and MC from the SR and region C are shown, since events are required to have $N_{\text{DV}} > 1$.

The full likelihood function is given by:

$$\mathcal{L}(\mu, \theta) = \prod_{i \in \{A,B,C,D\}} \left(\prod_{j \in i} P\left(N^{\text{Obs}}_{i,j} | N^{\text{Exp}}_{i,j}(p_0, p_1, \mu)\right) \right) \times \left(G\left(\alpha^{\text{Sig}}_i, \sigma^{\text{Sig}} | 0, 1\right) \right) \times \prod_{k=1}^{3} G\left(\alpha_k, \sigma_k | 0, 1\right) \tag{6}$$

where P represents the Poisson probabilities, and G are the Gaussian constraints on the systematic uncertainties, with α and σ the mean and standard deviations, respectively. The set of free parameters, other than the signal strength, is given by $\theta = \{p_0, p_1, N^{\text{Exp}}_{B,j}, N^{\text{Exp}}_{D,j}, \alpha^{\text{Sig}}_i, \alpha_k\}$.

The four signal systematic uncertainties (jet, track and vertex, pile-up, and PTF) are combined, but kept decorrelated across the four ABCD regions; the standard deviation of the Gaussian constraint (σ^{Sig}) is set to the same value across the

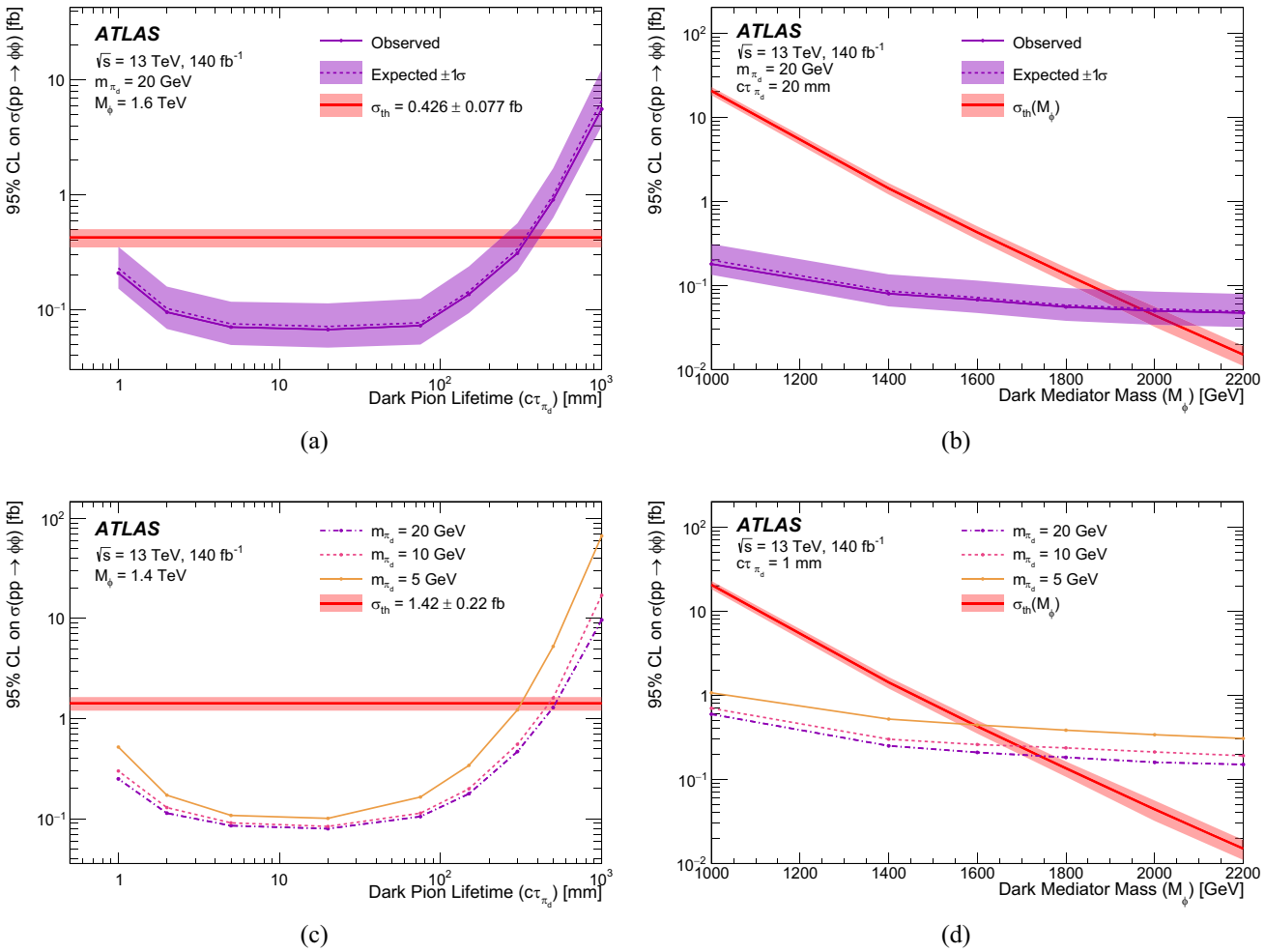

Fig. 6 95% CL upper limits as a function of (left) $c\tau_{\pi_d}$ and (right) M_ϕ. The upper plots show the expected and observed limits on $\sigma(pp \to \phi^\dagger\phi)$ for $m_{\pi_d} = 20$ GeV: **(a)** using $M_\phi = 1.6$ TeV and **(b)** using $c\tau_{\pi_d} = 20$ mm. The lower plots show a comparison of the observed limits for all three dark pion masses: **(c)** using $M_\phi = 1.4$ TeV, and **(d)** using $c\tau_{\pi_d} = 1$ mm. The mediator mass-dependent theoretical cross-section is given with the band corresponding to the uncertainty from NNLL- FAST

four regions (set by the combined systematic uncertainty), but the mean (α^{Sig}) is allowed to float independently in each region. This allows for different systematic uncertainty values in each region of the ABCD plane. The three other systematic uncertainties, one for the luminosity uncertainty, and two for the background estimate uncertainty (which are applied only to region A), are included as individual nuisance parameters. In these cases, the Gaussian terms are correlated across the full ABCD plane giving only a single value for the mean of each term, while the standard deviations are set by the corresponding systematic uncertainties.

The test statistic is defined using the profile likelihood ratio whose probability distribution is determined with the asymptotic approximation [74], and which gives a signal strength that is strictly positive. The likelihood implementation is handled by the `xRooFit` package.

Upper limits at the 95% confidence level (CL) are set on the pair-production cross-section for each signal hypothesis using the CL_s method [75]. Figure 6 shows the upper limit on $\sigma(pp \to \phi^\dagger\phi)$ at 95% confidence level as either a function of $c\tau_{\pi_d}$ or M_ϕ. In general, for a given combination of M_ϕ and $c\tau_{\pi_d}$, the sensitivity improves slightly with increasing m_{π_d}, as can be seen in Figs. 6c, d. The limits are strictest for intermediate dark pion lifetimes in the range 2 mm $< c\tau_{\pi_d} <$ 100 mm, but sensitivity decreases for $c\tau_{\pi_d} > 100$ mm due to the reduction in tracking and vertexing efficiency at large radii. Similarly, the limits weaken for $c\tau_{\pi_d} < 2$ mm due to the strict requirements on reconstructed DVs, and dark pions producing jets with larger prompt track fractions. This results in more Standard Model-like minPTF distributions, which is the strongest variable in the event-level BDT. The limits have only a weak dependence on M_ϕ, getting stronger at higher mediator masses.

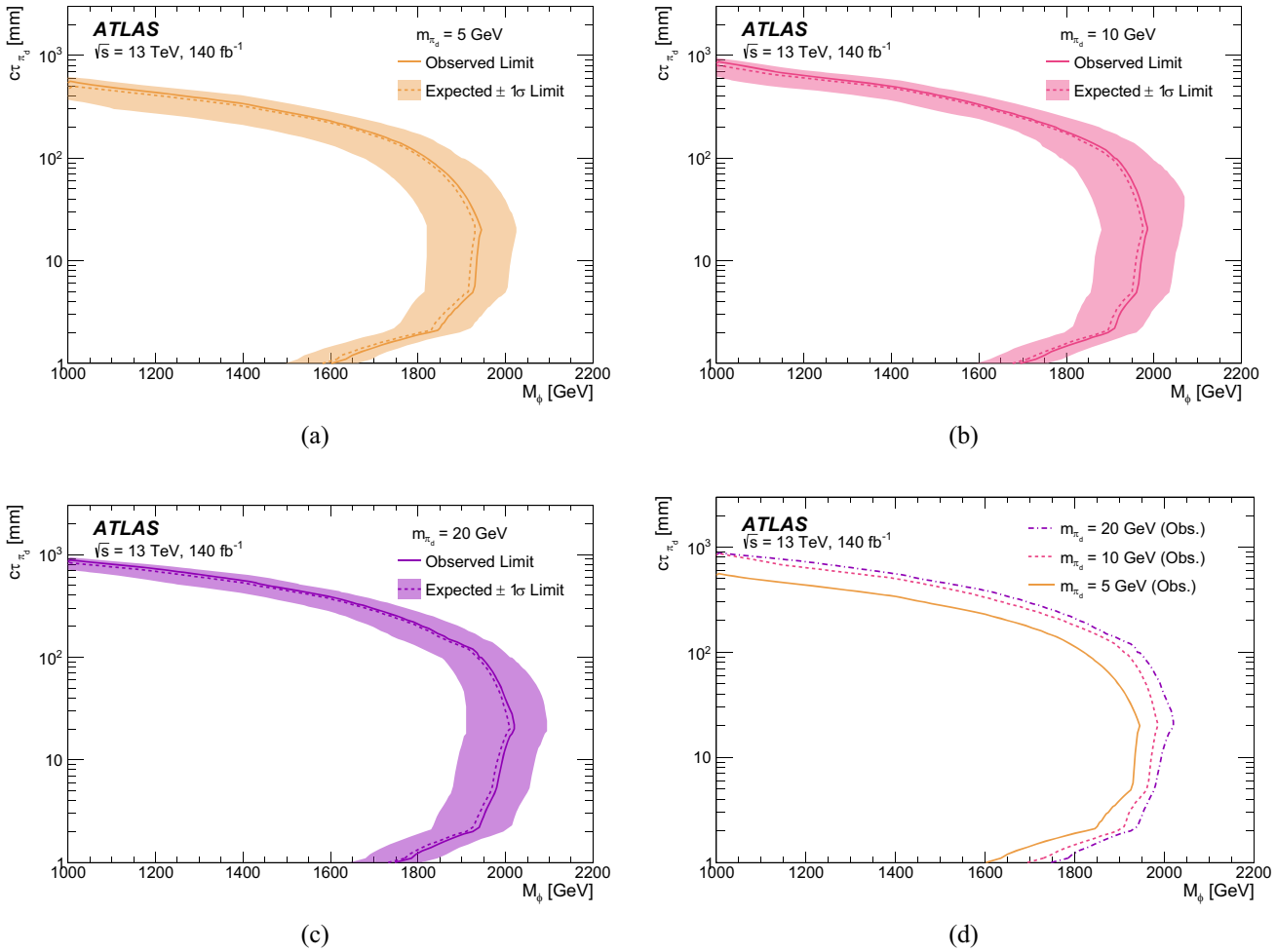

Fig. 7 95% CL exclusion contours as a function of M_ϕ and $c\tau_{\pi_d}$. The expected and observed limits on $\sigma(pp \to \phi^\dagger\phi)$ are shown for **(a)** $m_{\pi_d} = 5$ GeV, **(b)** $m_{\pi_d} = 10$ GeV, and **(c)** $m_{\pi_d} = 20$ GeV. A comparison of the observed limits is given in **(d)** for each of the three dark pion masses

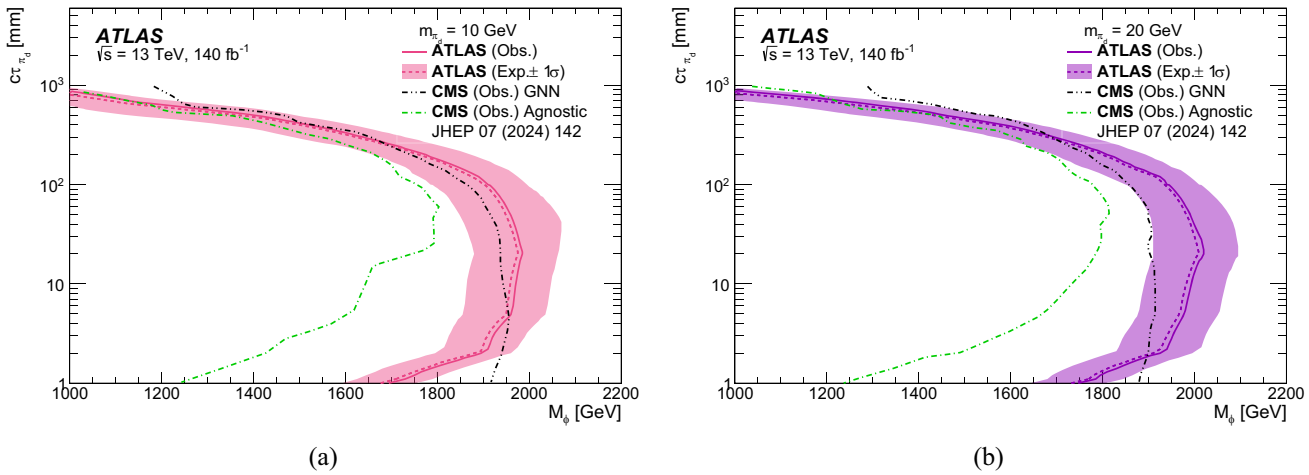

Fig. 8 Comparison of the 95% CL exclusion contours between ATLAS and CMS [28] for **(a)** models with $m_{\pi_d} = 10$ GeV and **(b)** models with $m_{\pi_d} = 20$ GeV. The expected and observed limits are shown for ATLAS, while only the observed limits in both the model agnostic and GNN cases are included for CMS. The expected limits from the CMS result are omitted, but are, in general, very close to the CMS observed limits

Exclusion contours based on the expected and observed limits on $\sigma(pp \to \phi^{\dagger}\phi)$ as a function of M_{ϕ} and $c\tau_{\pi_d}$ are shown for $m_{\pi_d} = 5, 10$ and 20 GeV in Figs. 7a–c, respectively. Figure 7d gives a comparison of the exclusion contours based on the observed limits for the three dark pion masses. For models with $c\tau_{\pi_d} = 20$ mm, the production cross-section is excluded for ϕ masses up to $M_{\phi} = 1.95$ TeV, 1.99 TeV, and 2.00 TeV for $m_{\pi_d} = 5,\ 10,\ 20$ GeV, respectively. For $M_{\phi} = 1$ TeV, dark pion lifetimes up to about 880 mm are excluded for $m_{\pi_d} = 10, 20$ GeV and up to about 530 mm for $m_{\pi_d} = 5$ GeV. The cutoff in the exclusion contours at $M_{\phi} > 2$ TeV is due to the rapidly falling theoretical cross sections, which become inaccessible with the current dataset.

This analysis is able to probe cross-sections that are a factor of two smaller than those in the four jet topology of the bifundamental scalar interpretation in the ATLAS Run 3 search [29], which is more optimised for the Z' scenario.

Figure 8 shows the comparison between the results of this analysis, with those from the corresponding CMS search [28]. CMS included two methods of tagging emerging jets: a *model agnostic* version based on track displacement variables, and an ML-based Graph Neural Network (GNN) tagger. The GNN sets stricter limits at very low and very high proper lifetimes, while this search is more sensitive for intermediate lifetimes ($2 - 300$ mm).

10 Conclusion

This paper presents a search for emerging jets, a detector signature arising from a strongly self-interacting dark sector, using 140 fb^{-1} of data from proton–proton collisions at $\sqrt{s} = 13$ TeV, collected by the ATLAS detector at the LHC between 2015 and 2018. The search uses a two-stage boosted decision tree: the first trained on jet-level variables, and the second using event-level observables to select emerging-jet-like events from a wide model space. The Standard Model background is estimated using a fully data-driven approach. No excess above this estimate is observed.

Upper limits on the pair-production cross-section of heavy scalar mediators are set at the 95% confidence level. Mediator masses up to 2 TeV are excluded for dark pions with proper decay lengths of 20 mm and a dark pion mass of 20 GeV. This search complements the larger experimental efforts of the ATLAS collaboration looking for dark QCD, and is competitive with the recent results from both CMS and ATLAS, in some cases setting the strictest limits to date on the pair-production of a new scalar mediator.

Acknowledgements We thank CERN for the very successful operation of the LHC and its injectors, as well as the support staff at CERN and at our institutions worldwide without whom ATLAS could not be operated efficiently. The crucial computing support from all WLCG partners is acknowledged gratefully, in particular from CERN, the ATLAS Tier-1 facilities at TRIUMF/SFU (Canada), NDGF (Denmark, Norway, Sweden), CC-IN2P3 (France), KIT/GridKA (Germany), INFN-CNAF (Italy), NL-T1 (Netherlands), PIC (Spain), RAL (UK) and BNL (USA), the Tier-2 facilities worldwide and large non-WLCG resource providers. Major contributors of computing resources are listed in [76]. We gratefully acknowledge the support of ANPCyT, Argentina; YerPhI, Armenia; ARC, Australia; BMWFW and FWF, Austria; ANAS, Azerbaijan; CNPq and FAPESP, Brazil; NSERC, NRC and CFI, Canada; CERN; ANID, Chile; CAS, MOST and NSFC, China; Minciencias, Colombia; MEYS CR, Czech Republic; DNRF and DNSRC, Denmark; IN2P3-CNRS and CEA-DRF/IRFU, France; SRNSFG, Georgia; BMFTR, HGF and MPG, Germany; GSRI, Greece; RGC and Hong Kong SAR, China; ICHEP and Academy of Sciences and Humanities, Israel; INFN, Italy; MEXT and JSPS, Japan; CNRST, Morocco; NWO, Netherlands; RCN, Norway; MNiSW, Poland; FCT, Portugal; MNE/IFA, Romania; MSTDI, Serbia; MSSR, Slovakia; ARIS and MVZI, Slovenia; DSI/NRF, South Africa; MICIU/AEI, Spain; SRC and Wallenberg Foundation, Sweden; SERI, SNSF and Cantons of Bern and Geneva, Switzerland; NSTC, Taipei; TENMAK, Türkiye; STFC/UKRI, United Kingdom; DOE and NSF, United States of America. Individual groups and members have received support from BCKDF, CANARIE, CRC and DRAC, Canada; CERN-CZ, FORTE and PRIMUS, Czech Republic; COST, ERC, ERDF, Horizon 2020, ICSC-NextGenerationEU and Marie Skłodowska-Curie Actions, European Union; Investissements d'Avenir Labex, Investissements d'Avenir Idex and ANR, France; DFG and AvH Foundation, Germany; Herakleitos, Thales and Aristeia programmes co-financed by EU-ESF and the Greek NSRF, Greece; BSF-NSF and MINERVA, Israel; NCN and NAWA, Poland; La Caixa Banking Foundation, CERCA Programme Generalitat de Catalunya and PROMETEO and GenT Programmes Generalitat Valenciana, Spain; Göran Gustafssons Stiftelse, Sweden; The Royal Society and Leverhulme Trust, United Kingdom. In addition, individual members wish to acknowledge support from CERN: European Organization for Nuclear Research (CERN DOCT); Chile: Agencia Nacional de Investigación y Desarrollo (FONDECYT 1230812, FONDECYT 1240864, Fondecyt 3240661, Fondecyt Regular 1240721); China: Chinese Ministry of Science and Technology (MOST-2023YFA1605700, MOST-2023YFA1609300), National Natural Science Foundation of China (NSFC-12175119, NSFC 12275265); Czech Republic: Czech Science Foundation (GACR-24-11373S), Ministry of Education Youth and Sports (ERC-CZ-LL2327, FORTE CZ.02.01.01/00/22_008/0004632), PRIMUS Research Programme (PRIMUS/21/SCI/017); EU: H2020 European Research Council (ERC-101002463); European Union: European Research Council (BARD No. 101116429, ERC-948254, ERC 101089007), European Regional Development Fund (HE COFUND GA No.101081355, ERDF), European Union, Future Artificial Intelligence Research (FAIR-NextGenerationEU PE00000013), Italian Center for High Performance Computing, Big Data and Quantum Computing (ICSC, NextGenerationEU); France: Agence Nationale de la Recherche (ANR-21-CE31-0013, ANR-21-CE31-0022, ANR-22-EDIR-0002, ANR-24-CE31-0504-01); Germany: Deutsche Forschungsgemeinschaft (DFG-469666862, DFG-CR 312/5-2); China: Research Grants Council (GRF); Italy: Istituto Nazionale di Fisica Nucleare (ICSC, NextGenerationEU), Ministero dell'Università e della Ricerca (NextGenEU 153D23001490006 M4C2.1.1, NextGenEU I53D23000820006 M4C2.1.1, NextGenEU I53D23001490006 M4C2.1.1, SOE2024_0000023); Japan: Japan Society for the Promotion of Science (JSPS KAKENHI JP22H01227, JSPS KAKENHI JP22H04944, JSPS KAKENHI JP22KK0227, JSPS KAKENHI JP24K23939, JSPS KAKENHI JP24KK0251, JSPS KAKENHI JP25H00650, JSPS KAKENHI JP25H01291, JSPS KAKENHI JP25K01023); Norway: Research Council of Norway (RCN-314472); Poland: Ministry of Science and Higher Education (IDUB AGH, POB8, D4 no 9722), Polish National Science Centre (NCN 2021/42/E/ST2/00350, NCN OPUS 2023/51/B/ST2/02507, NCN UMO-2019/34/E/ST2/00393, UMO-2022/47/O/ST2/00148, UMO-2023/49/B/ST2/04085, UMO-2023/51/

B/ST2/00920, UMO-2024/53/N/ST2/00869); Portugal: Foundation for Science and Technology (FCT); Spain: Generalitat Valenciana (ASFAE/2022/008), Ministry of Science and Innovation (MCIN and NextGenEU PCI2022-135018-2, MICIN and FEDER PID2021-125273NB, RYC2019-028510-I, RYC2020-030254-I, RYC2021-031273-I, RYC2022-038164-I), Ministerio de Ciencia, Innovación y Universidades/Agencia Estatal de Investigación (PID2022-142604OB-C22); Sweden: Carl Trygger Foundation (Carl Trygger Foundation CTS 22:2312), Swedish Research Council (Swedish Research Council 2023-04654, VR 2021-03651, VR 2022-03845, VR 2022-04683, VR 2023-03403, VR 2024-05451), Knut and Alice Wallenberg Foundation (KAW 2018.0458, KAW 2022.0358, KAW 2023.0366); Switzerland: Swiss National Science Foundation (SNSF-PCEFP2_194658); United Kingdom: Royal Society (NIF-R1-231091); United States of America: U.S. Department of Energy (ECA DE-AC02-76SF00515), Neubauer Family Foundation.

Data availability statement This manuscript has no associated data. [Author's' comment: The public release of data supporting the findings of this article will follow the CERN Open Data Policy [76]. The values of relevant plots and tables associated with this article are stored in HEPData (https://www.hepdata.net/record/ins3069355 for this article).]

Code availability statement This manuscript has no associated code/software. [Author's comment: The ATLAS Collaboration's Athena software, including the configuration of the event generators, is open source (http://gitlab.cern.ch/atlas/athena).]

Open Access This article is licensed under a Creative Commons Attribution 4.0 International License, which permits use, sharing, adaptation, distribution and reproduction in any medium or format, as long as you give appropriate credit to the original author(s) and the source, provide a link to the Creative Commons licence, and indicate if changes were made. The images or other third party material in this article are included in the article's Creative Commons licence, unless indicated otherwise in a credit line to the material. If material is not included in the article's Creative Commons licence and your intended use is not permitted by statutory regulation or exceeds the permitted use, you will need to obtain permission directly from the copyright holder. To view a copy of this licence, visit http://creativecommons.org/licenses/by/4.0/.
Funded by SCOAP[3].

A Cut-Based analysis

A cut-based version of the analysis was performed, but not optimized to the same degree as the BDT-based analysis. As such, it does not achieve the same sensitivity as the BDT, but it does provide results which are easier for theorists to reinterpret.

The analysis requires the same event selections as described in Sect. 5, and only differs in the choice of variables used in the ABCD plane for the background estimation. Instead of using the BDT response, the cut-based analysis uses the minimum prompt track fraction of the four highest p_T jets (minPTF), which is one of the best separating variables used in the BDT training. A comparison of the minPTF between Data and three example signal samples is shown in Fig. 9.

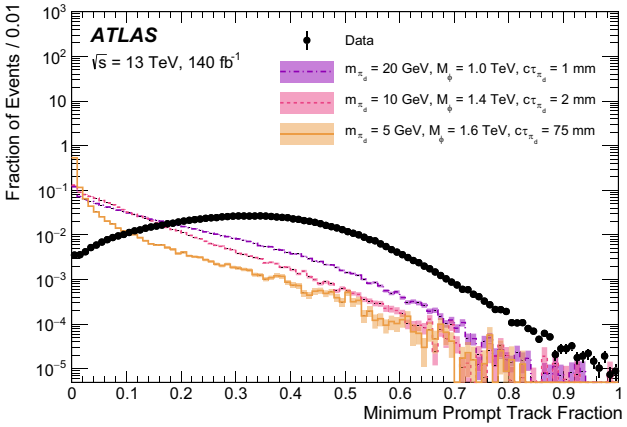

Fig. 9 Normalized minPTF distribution in data, with three selected signal samples for comparison

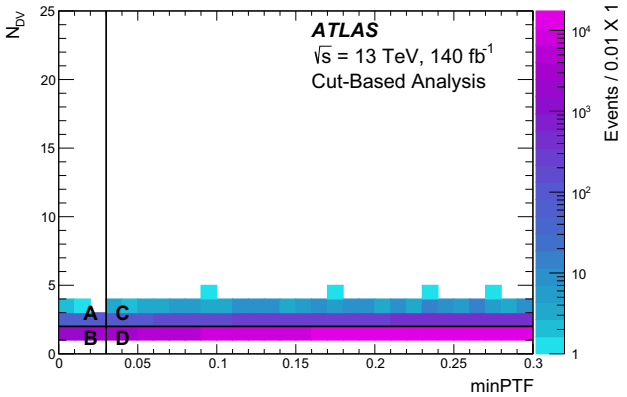

Fig. 10 Distribution of data events in the ABCD plane defined for the Cut-Based analysis, using the minimum prompt track fraction (minPTF) of the four highest p_T jets on the x-axis, and the displaced vertex multiplicity on the y-axis. The cuts used to define the four regions are at minPTF $= 0.03$ and $N_{\text{DV}} = 2$. The four regions are labeled accordingly

Table 6 Predicted number of background events, including statistical and systematic uncertainties, and observed event yield in the Cut-Based SR

Cut-based analysis: event yield in the SR	
Prediction	227 ± 10 (stat.) ± 1 (syst.)
Observed Yield	219

The ABCD plane is constructed using minPTF and the number of jet-matched displaced vertices in the event (N_{DV}). The cuts used to define the signal region are minPTF ≤ 0.03 and $N_{\text{DV}} \geq 2$. In order to aid the background estimation method, which is the same as described in Sect. 7, minPTF is restricted to the region less than 0.3. The distribution of data events within the ABCD plane are shown in Fig. 10.

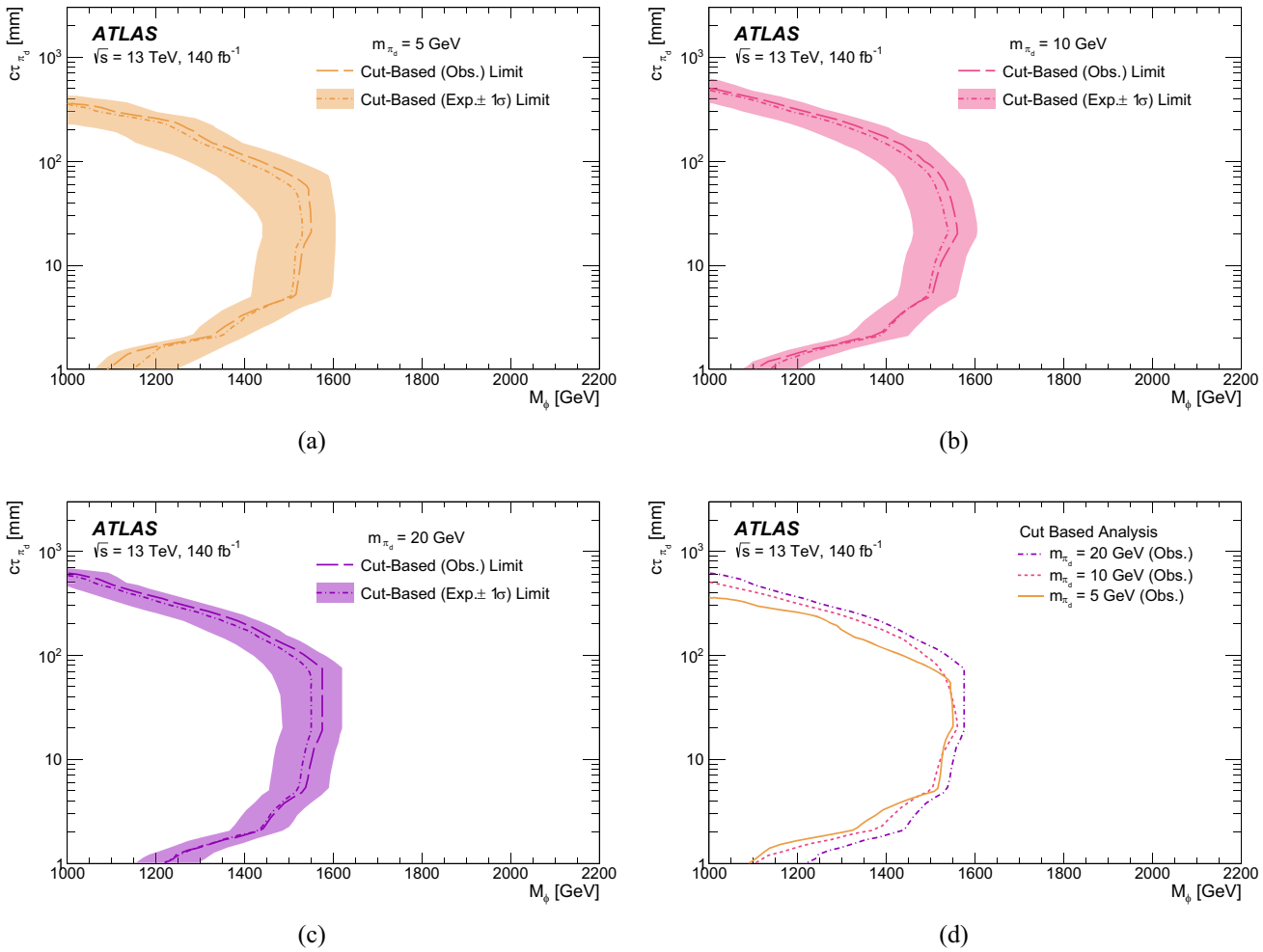

Fig. 11 95% CL exclusion contours as a function of M_ϕ and $c\tau_{\pi_d}$ for the Cut-Based analysis. The expected and observed limits on $\sigma(pp \to \phi^\dagger \phi)$ are shown for **(a)** $m_{\pi_d} = 5$ GeV, **(b)** $m_{\pi_d} = 10$ GeV, and **(c)** $m_{\pi_d} = 20$ GeV. A comparison of the observed limits is given in **(d)** for each of the three dark pion masses

An extrapolated linear fit based on the modified ABCD method was used to produce a prediction of the background contribution in the SR. The predicted and observed yield in region A are given in Table 6. No excess above the SM background prediction is observed

Using the same statistical machinery as described in Sect. 9, limits at the 95% confidence level are produced for the Cut-Based analysis. Exclusion contours as a function of M_ϕ and $c\tau_{\pi_d}$ are shown for $m_{\pi_d} = 5, 10$ and 20 GeV in Fig. 11a–c respectively. A comparison of the observed limits for all three dark pion masses is shown in Fig. 11d

The Cut-Based analysis excludes a much smaller region of phase-space as compared to the BDT-based analysis, which speaks to the enhanced separating power that the BDT response has over any of the individual training variables. Comparisons between the Cut-Based and BDT-based analyses are shown in Fig. 12 for each of the dark pion masses individually.

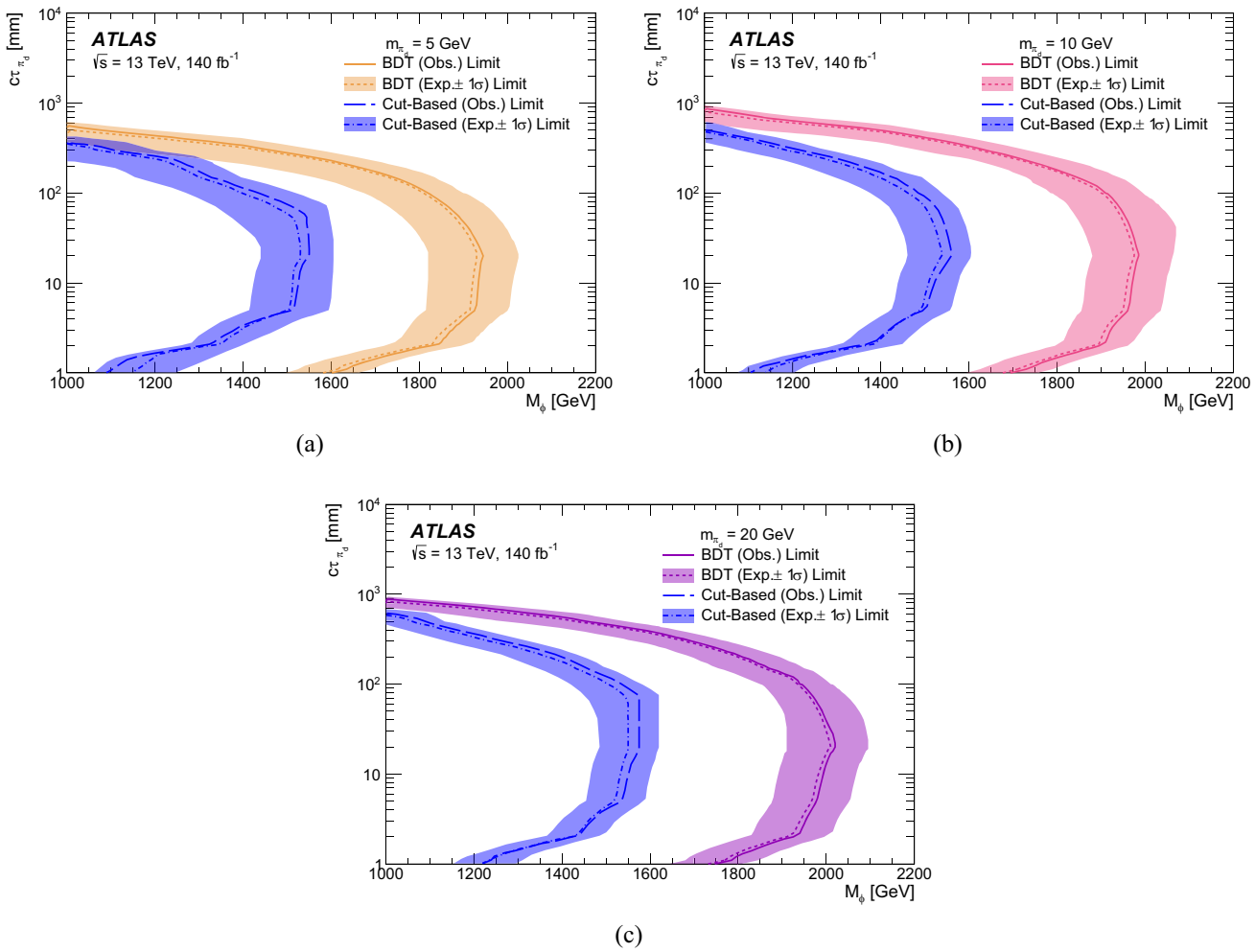

Fig. 12 Comparison of observed and expected 95% CL limits of the Cut-Based analysis against the corresponding BDT-based analysis. Limits on $\sigma(pp \to \phi^{\dagger}\phi)$ are shown as a function of M_{ϕ} and $c\tau_{\pi_d}$ for **(a)** $m_{\pi_d} = 5$ GeV, **(b)** $m_{\pi_d} = 10$ GeV, and **(c)** $m_{\pi_d} = 20$ GeV

References

1. V.C. Rubin, W.K. Ford Jr., N. Thonnard, Rotational properties of 21 SC galaxies with a large range of luminosities and radii, from NGC 4605 ($R = 4$ kpc) to UGC 2885 ($R = 122$ kpc). ApJ **238**, 471 (1980). https://doi.org/10.1086/158003
2. M. Persic, P. Salucci, F. Stel, The universal rotation curve of spiral galaxies—I. The dark matter connection, MNRAS 281 (1996) 27, https://doi.org/10.48550/arXiv.astro-ph/9506004. arXiv:astro-ph/9506004
3. D. Clowe et al., A direct empirical proof of the existence of dark matter. ApJ **648**, L109 (2006). https://doi.org/10.1086/508162. arXiv:astro-ph/0608407
4. D.S. Collaboration, DarkSide-50 532-day dark matter search with low-radioactivity argon. Phys. Rev. D **98**, 102006 (2018). https://doi.org/10.1103/physrevd.98.102006. arXiv:1802.07198 [astro-ph]
5. S.C.D.M.S. Collaboration, Search for low-mass dark matter with CDMSlite using a profile likelihood fit. Phys. Rev. D **99**, 062001 (2019). https://doi.org/10.1103/physrevd.99.062001. arXiv:1808.09098 [astro-ph]
6. P.I.C.O. Collaboration, Dark matter search results from the complete exposure of the PICO-60 C_3F_8 bubble chamber. Phys. Rev. D **100**, 022001 (2019). https://doi.org/10.1103/physrevd.100.022001. arXiv:1902.04031 [astro-ph]
7. XENON Collaboration, Search for coherent elastic scattering of solar ^{8}B neutrinos in the XENON1T Dark Matter Experiment. Phys. Rev. Lett. 126 (2021) 091301, https://doi.org/10.1103/physrevlett.126.091301. arXiv:2012.02846 [hep-ex]
8. M. Lai (on behalf of the DEAP-3600 Collaboration), Recent results from DEAP-3600, JINST 18 (2023) C02046, https://doi.org/10.1088/1748-0221/18/02/c02046. arXiv:2302.14484 [hep-ex]
9. PandaX Collaboration, Dark matter search results from 1.54 Tonne · year exposure of PandaX-4T. Phys. Rev. Lett. **134**, 011805 (2025). https://doi.org/10.1103/physrevlett.134.011805. arXiv:2408.00664 [hep-ex]
10. ATLAS Collaboration, Exploration at the high-energy frontier: ATLAS Run 2 searches investigating the exotic jungle beyond the Standard Model. Phys. Rep. **1116**, 301 (2025). https://doi.org/10.1016/j.physrep.2024.10.001. arXiv:2403.09292 [hep-ex]
11. C.M.S. Collaboration, Dark sector searches with the CMS experiment. Phys. Rep. **1115**, 448 (2025). https://doi.org/10.1016/j.physrep.2024.09.013. arXiv:2405.13778 [hep-ex]

12. LZ Collaboration, Dark matter search results from 4.2 tonne-years of exposure of the LUX-ZEPLIN (LZ) Experiment. Phys. Rev. Lett. **135**, 011802 (2025). https://doi.org/10.1103/4dyc-z8zf. arXiv:2410.17036 [hep-ex]
13. M.J. Strassler, K.M. Zurek, Echoes of a hidden valley at hadron colliders. Phys. Lett. B **651**, 374 (2007). https://doi.org/10.1016/j.physletb.2007.06.055. arXiv:hep-ph/0604261
14. M.J. Strassler, K.M. Zurek, Discovering the Higgs through highly-displaced vertices. Phys. Lett. B **661**, 263 (2008). https://doi.org/10.1016/j.physletb.2008.02.008. arXiv:hep-ph/0605193
15. T. Han, Z. Si, K.M. Zurek, M.J. Strassler, Phenomenology of hidden valleys at hadron colliders. JHEP **07**, 008 (2008). https://doi.org/10.1088/1126-6708/2008/07/008. arXiv:0712.2041 [hep-ph]
16. Y. Bai, P. Schwaller, Scale of dark QCD. Phys. Rev. D **89**, 063522 (2014). https://doi.org/10.1103/physrevd.89.063522. arXiv:1306.4676 [hep-ph]
17. H. Beauchesne, E. Bertuzzo, G. Grilli di Cortona, Dark matter in Hidden Valley models with stable and unstable light dark mesons. JHEP **04**, 118 (2019). https://doi.org/10.1007/jhep04(2019)118. arXiv:1809.10152 [hep-ph]
18. G. Albouy et al., Theory, phenomenology, and experimental avenues for dark showers: a Snowmass 2021 report. Eur. Phys. J. C **82**, 1132 (2022). https://doi.org/10.1140/epjc/s10052-022-11048-8. arXiv:2203.09503 [hep-ph]
19. M. Park, M. Zhang, Tagging a jet from a dark sector with jet substructures at colliders. Phys. Rev. D (2019). https://doi.org/10.1103/physrevd.100.115009. arXiv:1712.09279 [hep-ph]
20. T. Cohen, M. Lisanti, H.K. Lou, Semivisible jets: dark matter undercover at the LHC. Phys. Rev. Lett. (2015). https://doi.org/10.1103/physrevlett.115.171804. arXiv:1503.00009 [hep-ph]
21. P. Schwaller, D. Stolarski, A. Weiler, Emerging jets. JHEP **05**, 059 (2015). https://doi.org/10.1007/jhep05(2015)059. arXiv:1502.05409 [hep-ph]
22. ATLAS Collaboration, Search for non-resonant production of semi-visible jets using Run 2 data in ATLAS. Phys. Lett. B **848**, 138324 (2024). https://doi.org/10.1016/j.physletb.2023.138324. arXiv:2305.18037 [hep-ex]
23. ATLAS Collaboration, Search for new physics in final states with semivisible jets or anomalous signatures using the ATLAS detector. Phys. Rev. D **112**, 012021 (2025). https://doi.org/10.1103/44zp-mh1q. arXiv:2505.01634 [hep-ex]
24. C.M.S. Collaboration, Search for resonant production of strongly coupled dark matter in proton-proton collisions at 13 TeV. JHEP **06**, 156 (2022). https://doi.org/10.1007/JHEP06(2022)156. arXiv:2112.11125 [hep-ex]
25. ATLAS Collaboration, Search for resonant production of dark quarks in the dijet final state with the ATLAS detector, JHEP **02**, 128 (2024). https://doi.org/10.1007/JHEP02(2024)128. arXiv:2311.03944 [hep-ex]
26. ATLAS Collaboration, Search for long-lived, weakly interacting particles that decay to displaced hadronic jets in proton–proton collisions at $\sqrt{s} = 8TeV$ with the ATLAS detector. Phys. Rev. D **92**, 012010 (2015). https://doi.org/10.1103/PhysRevD.92.012010. arXiv:1504.03634 [hep-ex]
27. C.M.S. Collaboration, Search for new particles decaying to a jet and an emerging jet. JHEP **02**, 179 (2019). https://doi.org/10.1007/JHEP02(2019)179. arXiv:1810.10069 [hep-ex]
28. C.M.S. Collaboration, Search for dark QCD with emerging jets in proton–proton collisions at $\sqrt{s} = 13TeV$. JHEP **07**, 142 (2024). https://doi.org/10.1007/JHEP07(2024)142. arXiv:2403.01556 [hep-ex]
29. ATLAS Collaboration, Search for emerging jets in pp collisions at $\sqrt{s} = 13.6TeV$ with the ATLAS experiment. Rep. Prog. Phys. **88**, 097801 (2025). https://doi.org/10.1088/1361-6633/adfe17. arXiv:2505.02429 [hep-ex]
30. C. Arina et al., t-Channel dark matter models—a whitepaper. Eur. Phys. J. C **85**, 975 (2025). https://doi.org/10.1140/epjc/s10052-025-14635-7. arXiv:2504.10597 [hep-ph]
31. ATLAS Collaboration, The ATLAS Experiment at the CERN large hadron collider. JINST **3**, S08003 (2008). https://doi.org/10.1088/1748-0221/3/08/S08003
32. ATLAS Collaboration, ATLAS Insertable B-Layer: Technical Design Report, ATLAS-TDR-19; CERN-LHCC-2010-013, 2010, Addendum: ATLAS-TDR-19-ADD-1; CERN-LHCC-2012-009 (2012). https://cds.cern.ch/record/1291633. https://cds.cern.ch/record/1451888. Accessed 14 Oct 2025
33. B. Abbott et al., Production and integration of the ATLAS Insertable B-Layer. JINST **13**, T05008 (2018). https://doi.org/10.1088/1748-0221/13/05/T05008. arXiv:1803.00844 [physics.ins-det]
34. G. Avoni et al., The new LUCID-2 detector for luminosity measurement and monitoring in ATLAS. JINST **13**, P07017 (2018). https://doi.org/10.1088/1748-0221/13/07/P07017
35. ATLAS Collaboration, Performance of the ATLAS trigger system in. Eur. Phys. J. C **77**(2017), 317 (2015). https://doi.org/10.1140/epjc/s10052-017-4852-3. arXiv:1611.09661 [hep-ex]
36. ATLAS Collaboration, The ATLAS simulation infrastructure. Eur. Phys. J. C **70**, 823 (2010). https://doi.org/10.1140/epjc/s10052-010-1429-9. arXiv:1005.4568 [physics.ins-det]
37. ATLAS Collaboration, ATLAS data quality operations and performance for 2015–2018 data-taking. JINST **15**, P04003 (2020). https://doi.org/10.1088/1748-0221/15/04/P04003. arXiv:1911.04632 [physics.ins-det]
38. T. Sjöstrand et al., An introduction to PYTHIA 8.2. Comput. Phys. Commun. **191**, 159 (2015). https://doi.org/10.1016/j.cpc.2015.01.024. arXiv:1410.3012 [hep-ph]
39. NNPDF Collaboration, R.D. Ball et al., Parton distributions with LHC data. Nucl. Phys. B **867**, 244 (2013). https://doi.org/10.1016/j.nuclphysb.2012.10.003. arXiv:1207.1303 [hep-ph]
40. ATLAS Collaboration, ATLAS Pythia 8 tunes to 7 TeV data, ATL-PHYS-PUB-2014-021 (2014). https://cds.cern.ch/record/1966419. Accessed 14 Oct 2025
41. T. Sjöstrand, S. Mrenna, P. Skands, A brief introduction to PYTHIA 8.1. Comput. Phys. Commun. **178**, 852 (2008). https://doi.org/10.1016/j.cpc.2008.01.036. arXiv:0710.3820 [hep-ph]
42. ATLAS Collaboration, The Pythia 8 A3 tune description of ATLAS minimum bias and inelastic measurements incorporating the Donnachie–Landshoff diffractive model, ATL-PHYS-PUB-2016-017 (2016). https://cds.cern.ch/record/2206965. Accessed 14 Oct 2025
43. S. Agostinelli et al., Geant4—a simulation toolkit. Nucl. Instrum. Methods A **506**, 250 (2003). https://doi.org/10.1016/S0168-9002(03)01368-8
44. L. Carloni, T. Sjöstrand, Visible effects of invisible Hidden Valley radiation. JHEP **09**, 105 (2010). https://doi.org/10.1007/jhep09(2010)105. arXiv:1006.2911 [hep-ph]
45. W. Beenakker, C. Borschensky, M. Krämer, A. Kulesza, E. Laenen, NNLL-fast: predictions for coloured supersymmetric particle production at the LHC with threshold and Coulomb resummation. JHEP **12**, 133 (2016). https://doi.org/10.1007/jhep12(2016)133. arXiv:1607.07741 [hep-ph]
46. W. Beenakker et al., NNLL resummation for stop pair-production at the LHC. JHEP **05**, 153 (2016). https://doi.org/10.1007/jhep05(2016)153. arXiv:1601.02954 [hep-ph]
47. D.J. Gross, F. Wilczek, Ultraviolet behavior of non-abelian gauge theories. Phys. Rev. Lett. **30**, 1343 (1973). https://doi.org/10.1103/PhysRevLett.30.1343
48. H.D. Politzer, Reliable perturbative results for strong interactions? Phys. Rev. Lett. **30**, 1346 (1973). https://doi.org/10.1103/PhysRevLett.30.1346

49. ATLAS Collaboration, Multijet simulation for 13 TeV ATLAS Analyses, ATL-PHYS-PUB-2019-017 (2019). https://cds.cern.ch/record/2672252. Accessed 14 Oct 2025
50. P. Nason, A new method for combining NLO QCD with shower Monte Carlo algorithms. JHEP **11**, 040 (2004). https://doi.org/10.1088/1126-6708/2004/11/040. arXiv:hep-ph/0409146
51. S. Frixione, P. Nason, C. Oleari, Matching NLO QCD computations with parton shower simulations: the POWHEG method. JHEP **11**, 070 (2007). https://doi.org/10.1088/1126-6708/2007/11/070. arXiv:0709.2092 [hep-ph]
52. S. Alioli, P. Nason, C. Oleari, E. Re, A general framework for implementing NLO calculations in shower Monte Carlo programs: the POWHEG BOX. JHEP **06**, 043 (2010). https://doi.org/10.1007/JHEP06(2010)043. arXiv:1002.2581 [hep-ph]
53. ATLAS Collaboration, Study of top-quark pair modelling and uncertainties using ATLAS measurements at $\sqrt{s} = 13TeV$, ATL-PHYS-PUB-2020-023 (2020). https://cds.cern.ch/record/2730443. Accessed 14 Oct 2025
54. D.J. Lange, The EvtGen particle decay simulation package. Nucl. Instrum. Methods A **462**, 152 (2001). https://doi.org/10.1016/S0168-9002(01)00089-4
55. R. Frühwirth, Application of Kalman filtering to track and vertex fitting. Nucl. Instrum. Methods A **262**, 444 (1987). https://doi.org/10.1016/0168-9002(87)90887-4
56. ATLAS Collaboration, Performance of the reconstruction of large impact parameter tracks in the inner detector of ATLAS, ATL-PHYS-PUB-2017-014 (2017). https://cds.cern.ch/record/2275635. Accessed 14 Oct 2025
57. ATLAS Collaboration, Vertex Reconstruction Performance of the ATLAS Detector at $\sqrt{s} = 13TeV$, ATL-PHYS-PUB-2015-026 (2015). https://cds.cern.ch/record/2037717. Accessed 14 Oct 2025
58. ATLAS Collaboration, Performance of vertex reconstruction algorithms for detection of new long-lived particle decays within the ATLAS inner detector, ATL-PHYS-PUB-2019-013 (2019). https://cds.cern.ch/record/2669425. Accessed 14 Oct 2025
59. ATLAS Collaboration, Study of the material of the ATLAS inner detector for Run 2 of the LHC. JINST **12**, P12009 (2017). https://doi.org/10.1088/1748-0221/12/12/P12009. arXiv:1707.02826 [hep-ex]
60. ATLAS Collaboration, Topological cell clustering in the ATLAS calorimeters and its performance in LHC Run 1. Eur. Phys. J. C **77**, 490 (2017). https://doi.org/10.1140/epjc/s10052-017-5004-5. arXiv:1603.02934 [hep-ex]
61. ATLAS Collaboration, Jet energy scale measurements and their systematic uncertainties in proton–proton collisions at $\sqrt{s} = 13TeV$ with the ATLAS detector. Phys. Rev. D **96**, 072002 (2017). https://doi.org/10.1103/PhysRevD.96.072002. arXiv:1703.09665 [hep-ex]
62. ATLAS Collaboration, ATLAS flavour-tagging algorithms for the LHC Run 2 *pp* collision dataset. Eur. Phys. J. C **83**, 681 (2023). https://doi.org/10.1140/epjc/s10052-023-11699-1. arXiv:2211.16345 [physics.data-an]
63. ATLAS Collaboration, Operation of the ATLAS trigger system in Run 2. JINST **15**, P10004 (2020). https://doi.org/10.1088/1748-0221/15/10/P10004. arXiv:2007.12539 [physics.ins-det]
64. ATLAS Collaboration, The performance of the jet trigger for the ATLAS detector during data taking. Eur. Phys. J. C **76**(2016), 526 (2011). https://doi.org/10.1140/epjc/s10052-016-4325-0. arXiv:1606.07759 [hep-ex]
65. ATLAS Collaboration, Performance of the upgraded PreProcessor of the ATLAS Level-1 Calorimeter Trigger. JINST **15**, P11016 (2020). https://doi.org/10.1088/1748-0221/15/11/P11016. arXiv:2005.04179 [physics.ins-det]
66. A. Hoecker et al., TMVA—Toolkit for Multivariate Data Analysis (2009). arXiv:physics/0703039 [physics.data-an]
67. ATLAS Collaboration, Measurement of hadronic event shapes in $high-_{pT}$ multijet final states at $\sqrt{s} = 13TeV$ with the ATLAS detector. JHEP **01**, 188 (2021) [Erratum: JHEP 12 (2021) 053]. https://doi.org/10.1007/JHEP12(2021)053. arXiv:2007.12600 [hep-ex]
68. ATLAS Collaboration, Jet energy scale and resolution measured in proton–proton collisions at $\sqrt{s} = 13TeV$ with the ATLAS detector. Eur. Phys. J. C **81**, 689 (2021). https://doi.org/10.1140/epjc/s10052-021-09402-3. arXiv:2007.02645 [hep-ex]
69. ATLAS Collaboration, In situ calibration of large-radius jet energy and mass in $13TeV$ proton–proton collisions with the ATLAS detector. Eur. Phys. J. C **79**, 135 (2019). https://doi.org/10.1140/epjc/s10052-019-6632-8. arXiv:1807.09477 [hep-ex]
70. ATLAS Collaboration, Search for exotic decays of the Higgs boson into long-lived particles in *pp* collisions at $\sqrt{s} = 13TeV$ using displaced vertices in the ATLAS inner detector. JHEP **11**, 229 (2021). https://doi.org/10.1007/JHEP11(2021)229. arXiv:2107.06092 [hep-ex]
71. ATLAS Collaboration, Early inner detector tracking performance in the 2015 data at $\sqrt{s} = 13TeV$, ATL-PHYS-PUB-2015-051 (2015). https://cds.cern.ch/record/2110140. Accessed 14 Oct 2025
72. ATLAS Collaboration, Measurement of the inelastic proton–proton cross section at $\sqrt{s} = 13TeV$ with the ATLAS detector at the LHC. Phys. Rev. Lett. **117**, 182002 (2016). https://doi.org/10.1103/PhysRevLett.117.182002. arXiv:1606.02625 [hep-ex]
73. ATLAS Collaboration, Luminosity determination in *pp* collisions at $\sqrt{s} = 13\,TeV$ using the ATLAS detector at the LHC. Eur. Phys. J. C **83**, 982 (2023). https://doi.org/10.1140/epjc/s10052-023-11747-w. arXiv:2212.09379 [hep-ex]
74. G. Cowan, K. Cranmer, E. Gross, O. Vitells, Asymptotic formulae for likelihood-based tests of new physics. Eur. Phys. J. C (2011). https://doi.org/10.1140/epjc/s10052-011-1554-0. arXiv:1007.1727 [physics.data-an]
75. A.L. Read, Presentation of search results: the CL_s technique. J. Phys. G **28**, 2693 (2002). https://doi.org/10.1088/0954-3899/28/10/313
76. ATLAS Collaboration, ATLAS Computing Acknowledgements, ATL-SOFT-PUB-2025-001 (2025). https://cds.cern.ch/record/2922210. Accessed 14 Oct 2025

The ATLAS Collaboration*

G. Aad[103], E. Aakvaag[17], B. Abbott[122], S. Abdelhameed[118a], K. Abeling[55], N. J. Abicht[49], S. H. Abidi[30], M. Aboelela[45], A. Aboulhorma[36e], H. Abramowicz[156], Y. Abulaiti[119], B. S. Acharya[69a,69b,m], A. Ackermann[63a], C. Adam Bourdarios[4], L. Adamczyk[86a], S. V. Addepalli[148], M. J. Addison[102], J. Adelman[117], A. Adiguzel[22c], T. Adye[136], A. A. Affolder[138], Y. Afik[40], M. N. Agaras[13], A. Aggarwal[101], C. Agheorghiesei[28c], F. Ahmadov[39,ad], S. Ahuja[96], S. Ahuja[168], X. Ai[142b], G. Aielli[76a,76b], A. Aikot[168], M. Ait Tamlihat[36e], B. Aitbenchikh[36a], T. P. A. Åkesson[99], A. V. Akimov[150], D. Akiyama[173], N. N. Akolkar[25], S. Aktas[171], G. L. Alberghi[24b], J. Albert[170], U. Alberti[20], P. Albicocco[53], G. L. Albouy[60], S. Alderweireldt[52], Z. L. Alegria[123], M. Aleksa[37], I. N. Aleksandrov[39], C. Alexa[28b], T. Alexopoulos[10], F. Alfonsi[24b], M. Algren[56], M. Alhroob[172], B. Ali[134], H. M. J. Ali[92,w], S. Ali[32], S. W. Alibocus[93], M. Aliev[34c], G. Alimonti[71a], W. Alkakhi[55], C. Allaire[66], B. M. M. Allbrooke[151], D. R. Allen[123], J. S. Allen[102], J. F. Allen[52], P. P. Allport[21], A. Aloisio[72a,72b], F. Alonso[91], C. Alpigiani[141], Z. M. K. Alsolami[92], A. Alvarez Fernandez[101], M. Alves Cardoso[56], M. G. Alviggi[72a,72b], M. Aly[102], Y. Amaral Coutinho[82b], A. Ambler[105], C. Amelung[37], M. Amerl[102], C. G. Ames[110], T. Amezza[129], D. Amidei[107], B. Amini[54], K. Amirie[160], A. Amirkhanov[39], S. P. Amor Dos Santos[132a], K. R. Amos[168], D. Amperiadou[157], S. An[83], C. Anastopoulos[144], T. Andeen[11], J. K. Anders[93], A. C. Anderson[59], A. Andreazza[71a,71b], S. Angelidakis[9], A. Angerami[42], A. V. Anisenkov[39], A. Annovi[74a], C. Antel[37], E. Antipov[150], M. Antonelli[53], F. Anulli[75a], M. Aoki[83], T. Aoki[158], M. A. Aparo[151], L. Aperio Bella[48], M. Apicella[31], C. Appelt[156], A. Apyan[27], M. Arampatzi[10], S. J. Arbiol Val[87], C. Arcangeletti[53], A. T. H. Arce[51], J.-F. Arguin[109], S. Argyropoulos[157], J.-H. Arling[48], O. Arnaez[4], H. Arnold[150], G. Artoni[75a,75b], H. Asada[112], K. Asai[120], S. Asatryan[178], N. A. Asbah[37], R. A. Ashby Pickering[172], A. M. Aslam[96], K. Assamagan[30], R. Astalos[29a], K. S. V. Astrand[99], S. Atashi[164], R. J. Atkin[34a], H. Atmani[36f], P. A. Atmasiddha[130], K. Augsten[134], A. D. Auriol[41], V. A. Austrup[102], A. S. Avad[95], G. Avolio[37], K. Axiotis[56], A. Azzam[13], D. Babal[29b], H. Bachacou[137], K. Bachas[157,q], A. Bachiu[35], E. Bachmann[50], M. J. Backes[63a], A. Badea[40], T. M. Baer[107], P. Bagnaia[75a,75b], M. Bahmani[19], D. Bahner[54], K. Bai[125], J. T. Baines[136], L. Baines[95], O. K. Baker[177], E. Bakos[16], D. Bakshi Gupta[8], L. E. Balabram Filho[82b], V. Balakrishnan[122], R. Balasubramanian[4], E. M. Baldin[38], P. Balek[86a], E. Ballabene[24a,24b], F. Balli[137], L. M. Baltes[63a], W. K. Balunas[33], J. Balz[101], I. Bamwidhi[118b], E. Banas[87], M. Bandieramonte[131], A. Bandyopadhyay[25], S. Bansal[25], L. Barak[156], M. Barakat[48], E. L. Barberio[106], D. Barberis[18b], M. Barbero[103], M. Z. Barel[116], T. Barillari[111], M.-S. Barisits[37], T. Barklow[148], P. Baron[135], D. A. Baron Moreno[102], A. Baroncelli[62], A. J. Barr[128], J. D. Barr[97], F. Barreiro[100], J. Barreiro Guimarães da Costa[14], M. G. Barros Teixeira[132a], S. Barsov[38], F. Bartels[63a], R. Bartoldus[148], A. E. Barton[92], P. Bartos[29a], M. Baselga[49], S. Bashiri[87], A. Bassalat[66,b], M. J. Basso[161a], S. Bataju[45], R. Bate[169], R. L. Bates[59], S. Batlamous[100], M. Battaglia[138], D. Battulga[19], M. Bauce[75a,75b], M. Bauer[79], P. Bauer[25], L. T. Bayer[48], L. T. Bazzano Hurrell[31], J. B. Beacham[111], T. Beau[129], J. Y. Beaucamp[91], P. H. Beauchemin[163], P. Bechtle[25], H. P. Beck[20,p], K. Becker[172], A. J. Beddall[81], V. A. Bednyakov[39], C. P. Bee[150], L. J. Beemster[16], M. Begalli[82d], M. Begel[30], J. K. Behr[48], J. F. Beirer[37], F. Beisiegel[25], M. Belfkir[118b], G. Bella[156], L. Bellagamba[24b], A. Bellerive[35], C. D. Bellgraph[68], P. Bellos[21], K. Beloborodov[38], I. Benaoumeur[21], D. Benchekroun[36a], F. Bendebba[36a], Y. Benhammou[156], K. C. Benkendorfer[61], L. Beresford[48], M. Beretta[53], E. Bergeaas Kuutmann[166], N. Berger[4], B. Bergmann[134], J. Beringer[18a], G. Bernardi[5], C. Bernius[148], F. U. Bernlochner[25], A. Berrocal Guardia[13], T. Berry[96], P. Berta[135], A. Berti[132a], R. Bertrand[103], S. Bethke[111], A. Betti[75a,75b], A. J. Bevan[95], L. Bezio[56], N. K. Bhalla[54], S. Bharthuar[111], S. Bhatta[150], P. Bhattarai[148], Z. M. Bhatti[119], K. D. Bhide[54], V. S. Bhopatkar[123], R. M. Bianchi[131], G. Bianco[24a,24b], O. Biebel[110], M. Biglietti[77a], C. S. Billingsley[45], Y. Bimgdi[36f], M. Bindi[55], A. Bingham[176], A. Bingul[22b], C. Bini[75a,75b], G. A. Bird[33], M. Birman[174], M. Biros[135], S. Biryukov[151], T. Bisanz[49], E. Bisceglie[24a,24b], J. P. Biswal[136], D. Biswas[146], I. Bloch[48], A. Blue[59], U. Blumenschein[95], V. S. Bobrovnikov[39], L. Boccardo[57a,57b], M. Boehler[54], B. Boehm[171], D. Bogavac[13], A. G. Bogdanchikov[38], L. S. Boggia[129], V. Boisvert[96], P. Bokan[37], T. Bold[86a], M. Bomben[5], M. Bona[95], M. Boonekamp[137], A. G. Borbély[59], I. S. Bordulev[38], G. Borissov[92], D. Bortoletto[128], D. Boscherini[24b], M. Bosman[13], K. Bouaouda[36a], N. Bouchhar[168], L. Boudet[4], J. Boudreau[131], E. V. Bouhova-Thacker[92], D. Boumediene[41], R. Bouquet[57a,57b], A. Boveia[121], J. Boyd[37], D. Boye[30], I. R. Boyko[39], L. Bozianu[56], J. Bracinik[21], N. Brahimi[4], G. Brandt[176], O. Brandt[33], B. Brau[104],

J. E. Brau[125], R. Brener[174], L. Brenner[116], R. Brenner[166], S. Bressler[174], G. Brianti[78a,78b], D. Britton[59], D. Britzger[111], I. Brock[25], R. Brock[108], G. Brooijmans[42], A. J. Brooks[68], E. M. Brooks[161b], E. Brost[30], L. M. Brown[161a,170], L. E. Bruce[61], T. L. Bruckler[128], P. A. Bruckman de Renstrom[87], B. Brüers[48], A. Bruni[24b], G. Bruni[24b], D. Brunner[47a,47b], M. Bruschi[24b], N. Bruscino[75a,75b], T. Buanes[17], Q. Buat[141], D. Buchin[111], A. G. Buckley[59], O. Bulekov[81], B. A. Bullard[148], S. Burdin[93], C. D. Burgard[49], A. M. Burger[90], B. Burghgrave[8], O. Burlayenko[54], J. Burleson[167], J. C. Burzynski[147], E. L. Busch[42], V. Büscher[101], P. J. Bussey[59], O. But[25], J. M. Butler[26], C. M. Buttar[59], J. M. Butterworth[97], P. Butti[37], W. Buttinger[136], C. J. Buxo Vazquez[108], A. R. Buzykaev[39], S. Cabrera Urbán[168], L. Cadamuro[66], H. Cai[37], Y. Cai[24a,24b,113c], Y. Cai[113a], V. M. M. Cairo[37], O. Cakir[3a], N. Calace[37], P. Calafiura[18a], G. Calderini[129], P. Calfayan[35], L. Calic[99], G. Callea[59], L. P. Caloba[82b], D. Calvet[41], S. Calvet[41], R. Camacho Toro[129], S. Camarda[37], D. Camarero Munoz[27], P. Camarri[76a,76b], C. Camincher[170], M. Campanelli[97], A. Camplani[43], V. Canale[72a,72b], A. C. Canbay[3a], E. Canonero[96], J. Cantero[168], Y. Cao[167], F. Capocasa[27], M. Capua[44a,44b], A. Carbone[71a,71b], R. Cardarelli[76a], J. C. J. Cardenas[8], M. P. Cardiff[27], G. Carducci[44a,44b], T. Carli[37], G. Carlino[72a], J. I. Carlotto[13], B. T. Carlson[131,r], E. M. Carlson[170], J. Carmignani[93], L. Carminati[71a,71b], A. Carnelli[4], M. Carnesale[37], S. Caron[115], E. Carquin[139g], I. B. Carr[106], S. Carrá[73a,73b], G. Carratta[24a,24b], C. Carrion Martinez[168], A. M. Carroll[125], M. P. Casado[13,h], P. Casolaro[72a,72b], M. Caspar[48], W. R. Castiglioni[40], F. L. Castillo[4], L. Castillo Garcia[13], V. Castillo Gimenez[168], N. F. Castro[132a,132e], A. Catinaccio[37], J. R. Catmore[127], T. Cavaliere[4], V. Cavaliere[30], L. J. Caviedes Betancourt[23b], E. Celebi[81], S. Cella[37], V. Cepaitis[56], K. Cerny[124], A. S. Cerqueira[82a], A. Cerri[74a,am], L. Cerrito[76a,76b], F. Cerutti[18a], B. Cervato[71a,71b], A. Cervelli[24b], G. Cesarini[53], S. A. Cetin[81], P. M. Chabrillat[129], R. Chakkappai[66], S. Chakraborty[172], A. Chambers[61], J. Chan[18a], W. Y. Chan[158], J. D. Chapman[33], E. Chapon[137], B. Chargeishvili[154b], D. G. Charlton[21], C. Chauhan[135], Y. Che[113a], S. Chekanov[6], G. A. Chelkov[39,a], B. Chen[156], B. Chen[170], H. Chen[30], J. Chen[143a], J. Chen[147], M. Chen[128], S. Chen[88], S. J. Chen[113a], X. Chen[143a], X. Chen[15,ah], Z. Chen[62], C. L. Cheng[175], H. C. Cheng[64a], S. Cheong[148], A. Cheplakov[39], E. Cherepanova[116], R. Cherkaoui El Moursli[36e], E. Cheu[7], K. Cheung[65], L. Chevalier[137], V. Chiarella[53], G. Chiarelli[74a], G. Chiodini[70a], A. S. Chisholm[21], A. Chitan[28b], M. Chitishvili[168], M. V. Chizhov[39,s], K. Choi[11], Y. Chou[141], E. Y. S. Chow[115], K. L. Chu[174], M. C. Chu[64a], X. Chu[14,113c], Z. Chubinidze[53], J. Chudoba[133], J. J. Chwastowski[87], D. Cieri[111], K. M. Ciesla[86a], V. Cindro[94], A. Ciocio[18a], F. Cirotto[72a,72b], Z. H. Citron[174], M. Citterio[71a], D. A. Ciubotaru[28b], A. Clark[56], P. J. Clark[52], N. Clarke Hall[97], C. Clarry[160], S. E. Clawson[48], C. Clement[47a,47b], L. Clissa[24a,24b], Y. Coadou[103], M. Cobal[69a,69c], A. Coccaro[57b], R. F. Coelho Barrue[132a], R. Coelho Lopes De Sa[104], S. Coelli[71a], M. M. Cohen[130], L. S. Colangeli[160], B. Cole[42], P. Collado Soto[100], J. Collot[60], R. Coluccia[70a,70b], P. Conde Muiño[132a,132g], M. P. Connell[34c], S. H. Connell[34c], E. I. Conroy[128], M. Contreras Cossio[11], F. Conventi[72a,aj], A. M. Cooper-Sarkar[128], L. Corazzina[75a,75b], F. A. Corchia[24a,24b], A. Cordeiro Oudot Choi[141], L. D. Corpe[41], M. Corradi[75a,75b], F. Corriveau[105,ab], A. Cortes-Gonzalez[158], M. J. Costa[168], F. Costanza[4], D. Costanzo[144], J. Couthures[4], G. Cowan[96], K. Cranmer[175], L. Cremer[49], D. Cremonini[24a,24b], S. Crépé-Renaudin[60], F. Crescioli[129], T. Cresta[73a,73b], M. Cristinziani[146], M. Cristoforetti[78a,78b], E. Critelli[97], V. Croft[116], G. Crosetti[44a,44b], A. Cueto[100], H. Cui[97], Z. Cui[7], B. M. Cunnett[151], W. R. Cunningham[59], F. Curcio[168], J. R. Curran[52], M. J. Da Cunha Sargedas De Sousa[57a,57b], J. V. Da Fonseca Pinto[82b], C. Da Via[102], W. Dabrowski[86a], T. Dado[37], S. Dahbi[153], T. Dai[107], D. Dal Santo[20], C. Dallapiccola[104], M. Dam[43], G. D'amen[30], V. D'Amico[110], J. R. Dandoy[35], M. D'Andrea[57a,57b], D. Dannheim[37], G. D'anniballe[74a,74b], M. Danninger[147], V. Dao[150], G. Darbo[57b], S. J. Das[30], F. Dattola[48], S. D'Auria[71a,71b], A. D'Avanzo[72a,72b], T. Davidek[135], J. Davidson[172], I. Dawson[95], K. De[8], C. De Almeida Rossi[160], R. De Asmundis[72a], N. De Biase[48], S. De Castro[24a,24b], N. De Groot[115], P. de Jong[116], H. De la Torre[117], A. De Maria[113a], A. De Salvo[75a], U. De Sanctis[76a,76b], F. De Santis[70a,70b], A. De Santo[151], J. B. De Vivie De Regie[60], J. Debevc[94], D. V. Dedovich[39], J. Degens[93], A. M. Deiana[45], J. Del Peso[100], L. Delagrange[129], F. Deliot[137], C. M. Delitzsch[49], M. Della Pietra[72a,72b], D. Della Volpe[56], A. Dell'Acqua[37], L. Dell'Asta[71a,71b], M. Delmastro[4], C. C. Delogu[57a,57b], P. A. Delsart[60], S. Demers[177], M. Demichev[39], S. P. Denisov[38], H. Denizli[22a,l], M. G. Depala[93], L. D'Eramo[41], D. Derendarz[87], F. Derue[129], P. Dervan[93,*], A. M. Desai[1], K. Desch[25], F. A. Di Bello[74a,74b], A. Di Ciaccio[76a,76b], L. Di Ciaccio[4], A. Di Domenico[75a,75b], C. Di Donato[72a,72b], A. Di Girolamo[37], G. Di Gregorio[66], A. Di Luca[78a,78b], B. Di Micco[77a,77b], R. Di Nardo[77a,77b], K. F. Di Petrillo[40], M. Diamantopoulou[35], F. A. Dias[116], M. A. Diaz[139a,139b], A. R. Didenko[39], M. Didenko[168], S. D. Diefenbacher[18a], E. B. Diehl[107], S. Díez Cornell[48], C. Diez Pardos[146], C. Dimitriadi[149],

A. Dimitrievska[21], A. Dimri[150], Y. Ding[62], J. Dingfelder[25], T. Dingley[128], I.-M. Dinu[28b], S. J. Dittmeier[63b], F. Dittus[37], M. Divisek[135], B. Dixit[93], F. Djama[103], T. Djobava[154b], C. Doglioni[99,102], A. Dohnalova[29a], Z. Dolezal[135], K. Domijan[86a], K. M. Dona[40], M. Donadelli[82d], B. Dong[108], J. Donini[41], A. D'Onofrio[72a,72b], M. D'Onofrio[93], J. Dopke[136], A. Doria[72a], N. Dos Santos Fernandes[132a], I. A. Dos Santos Luz[82e], P. Dougan[102], M. T. Dova[91], A. T. Doyle[59], M. P. Drescher[55], E. Dreyer[174], I. Drivas-koulouris[10], M. Drnevich[119], D. Du[62], T. A. du Pree[116], Z. Duan[113a], M. Dubau[4], F. Dubinin[39], M. Dubovsky[29a], E. Duchovni[174], G. Duckeck[110], P. K. Duckett[97], O. A. Ducu[28b], D. Duda[52], A. Dudarev[37], M. M. Dudek[87], E. R. Duden[27], M. D'uffizi[102], L. Duflot[66], M. Dührssen[37], I. Duminica[28g], A. E. Dumitriu[28b], M. Dunford[63a], K. Dunne[47a,47b], A. Duperrin[103], H. Duran Yildiz[3a], A. Durglishvili[154b], G. I. Dyckes[18a], M. Dyndal[86a], B. S. Dziedzic[37], Z. O. Earnshaw[151], G. H. Eberwein[128], B. Eckerova[29a], S. Eggebrecht[55], E. Egidio Purcino De Souza[82e], G. Eigen[17], K. Einsweiler[18a], T. Ekelof[166], P. A. Ekman[99], S. El Farkh[36b], Y. El Ghazali[62], H. El Jarrari[105], A. El Moussaouy[36a], D. Elitez[37], M. Ellert[166], F. Ellinghaus[176], T. A. Elliot[96], N. Ellis[37], J. Elmsheuser[30], M. Elsawy[118a], M. Elsing[37], D. Emeliyanov[136], Y. Enari[83], S. Epari[109], D. Ernani Martins Neto[87], F. Ernst[37], M. Escalier[66], C. Escobar[168], E. Etzion[156], G. Evans[132a,132b], H. Evans[68], L. S. Evans[48], A. Ezhilov[38], S. Ezzarqtouni[36a], F. Fabbri[24a,24b], L. Fabbri[24a,24b], G. Facini[97], V. Fadeyev[138], R. M. Fakhrutdinov[38], D. Fakoudis[101], S. Falciano[75a], L. F. Falda Ulhoa Coelho[27], F. Fallavollita[111], G. Falsetti[44a,44b], J. Faltova[135], C. Fan[167], K. Y. Fan[64b], Y. Fan[14], Y. Fang[14,113c], M. Fanti[71a,71b], M. Faraj[69a,69b], Z. Farazpay[98], A. Farbin[8], A. Farilla[77a], K. Farman[153], J. N. Farr[177], M. S. Farrington[61], S. M. Farrington[52,136], F. Fassi[36e], D. Fassouliotis[9], L. Fayard[66], P. Federic[135], P. Federicova[133], O. L. Fedin[38,a], M. Feickert[175], L. Feligioni[103], D. E. Fellers[18a], C. Feng[142a], Y. Feng[14], Z. Feng[116], M. J. Fenton[164], L. Ferencz[48], B. Fernandez Barbadillo[92], P. Fernandez Martinez[67], M. J. V. Fernoux[103], J. Ferrando[92], A. Ferrari[166], P. Ferrari[115,116], R. Ferrari[73a], D. Ferrere[56], C. Ferretti[107], M. P. Fewell[1], D. Fiacco[75a,75b], F. Fiedler[101], P. Fiedler[134], S. Filimonov[39], M. S. Filip[28b,t], A. Filipčič[94], E. K. Filmer[161a], F. Filthaut[115], M. C. N. Fiolhais[132a,132c,c], L. Fiorini[168], W. C. Fisher[108], T. Fitschen[102], P. M. Fitzhugh[137], I. Fleck[146], P. Fleischmann[107], T. Flick[176], M. Flores[34d,ag], L. R. Flores Castillo[64a], M. Foll[127], F. M. Follega[78a,78b], N. Fomin[33], J. H. Foo[160], A. Formica[137], A. C. Forti[102], E. Fortin[37], A. W. Fortman[18a], L. Foster[18a], L. Fountas[9,i], D. Fournier[66], H. Fox[92], P. Francavilla[74a,74b], S. Francescato[61], S. Franchellucci[56], M. Franchini[24a,24b], S. Franchino[63a], D. Francis[37], L. Franco[48], L. Franconi[48], M. Franklin[61], G. Frattari[27], Y. Y. Frid[156], J. Friend[59], N. Fritzsche[37], A. Froch[56], D. Froidevaux[37], J. A. Frost[136], Y. Fu[108], S. Fuenzalida Garrido[139g], M. Fujimoto[150], K. Y. Fung[64a], E. Furtado De Simas Filho[82e], M. Furukawa[158], M. Fuste Costa[48], J. Fuster[168], A. Gaa[55], A. Gabrielli[24a,24b], A. Gabrielli[160], P. Gadow[37], G. Gagliardi[57a,57b], L. G. Gagnon[18a], S. Gaid[84b], S. Galantzan[156], J. Gallagher[1], E. J. Gallas[128], A. L. Gallen[166], B. J. Gallop[136], K. K. Gan[121], S. Ganguly[158], Y. Gao[52], A. Garabaglu[141], F. M. Garay Walls[139a,139b], C. García[168], A. Garcia Alonso[116], A. G. Garcia Caffaro[177], J. E. García Navarro[168], M. A. Garcia Ruiz[23b], M. Garcia-Sciveres[18a], G. L. Gardner[130], R. W. Gardner[40], N. Garelli[163], R. B. Garg[148], J. M. Gargan[33], C. A. Garner[160], C. M. Garvey[34a], V. K. Gassmann[163], G. Gaudio[73a], V. Gautam[13], P. Gauzzi[75a,75b], J. Gavranovic[94], I. L. Gavrilenko[132a], A. Gavrilyuk[38], C. Gay[169], G. Gaycken[125], E. N. Gazis[10], A. Gekow[121], C. Gemme[57b], M. H. Genest[60], A. D. Gentry[114], S. George[96], T. Geralis[46], A. A. Gerwin[122], P. Gessinger-Befurt[37], M. Ghani[172], K. Ghorbanian[95], A. Ghosal[146], A. Ghosh[164], A. Ghosh[7], B. Giacobbe[24b], S. Giagu[75a,75b], T. Giani[116], A. Giannini[62], S. M. Gibson[96], M. Gignac[138], D. T. Gil[86b], A. K. Gilbert[86a], B. J. Gilbert[42], D. Gillberg[35], G. Gilles[116], D. M. Gingrich[2,ai], M. P. Giordani[69a,69c], P. F. Giraud[137], G. Giugliarelli[69a,69c], D. Giugni[71a], F. Giuli[76a,76b], I. Gkialas[9,i], L. K. Gladilin[38], C. Glasman[100], M. Glazewska[20], R. M. Gleason[164], G. Glemža[48], M. Glisic[125], I. Gnesi[44b], Y. Go[30], M. Goblirsch-Kolb[37], B. Gocke[49], D. Godin[109], B. Gokturk[22a], S. Goldfarb[106], T. Golling[56], M. G. D. Gololo[34c], A. Golub[141], D. Golubkov[38], J. P. Gombas[108], A. Gomes[132a,132b], G. Gomes Da Silva[146], A. J. Gomez Delegido[37], R. Gonçalo[132a], L. Gonella[21], A. Gongadze[154c], F. Gonnella[21], J. L. Gonski[148], R. Y. González Andana[52], S. González de la Hoz[168], M. V. Gonzalez Rodrigues[48], R. Gonzalez Suarez[166], S. Gonzalez-Sevilla[56], L. Goossens[37], B. Gorini[37], E. Gorini[70a,70b], A. Gorišek[94], T. C. Gosart[130], A. T. Goshaw[51], M. I. Gostkin[39], S. Goswami[123], C. A. Gottardo[37], S. A. Gotz[110], M. Gouighri[36b], A. G. Goussiou[141], N. Govender[34c], R. P. Grabarczyk[128], I. Grabowska-Bold[86a], K. Graham[35], E. Gramstad[127], S. Grancagnolo[70a,70b], C. M. Grant[1], P. M. Gravila[28f], F. G. Gravili[70a,70b], H. M. Gray[18a], M. Greco[111], M. J. Green[1], C. Grefe[25], A. S. Grefsrud[17], I. M. Gregor[48], K. T. Greif[164], P. Grenier[148], S. G. Grewe[111], A. A. Grillo[138], K. Grimm[32], S. Grinstein[13,x],

J.-F. Grivaz[66], E. Gross[174], J. Grosse-Knetter[55], L. H. Grossman[18b], L. Guan[107], G. Guerrieri[37], R. Guevara[127], R. Gugel[101], J. A. M. Guhit[107], A. Guida[19], E. Guilloton[172], S. Guindon[37], F. Guo[14,113c], J. Guo[143a], L. Guo[48], L. Guo[113b,v], Y. Guo[107], Y. Guo[42], A. Gupta[49], R. Gupta[131], S. Gupta[27], S. Gurbuz[25], S. S. Gurdasani[48], G. Gustavino[75a,75b], P. Gutierrez[122], L. F. Gutierrez Zagazeta[130], M. Gutsche[50], C. Gutschow[97], C. Gwenlan[128], C. B. Gwilliam[93], E. S. Haaland[127], A. Haas[119], M. Habedank[59], C. Haber[18a], H. K. Hadavand[8], A. Haddad[41], A. Hadef[50], A. I. Hagan[92], J. J. Hahn[146], E. H. Haines[97], M. Haleem[171], J. Haley[123], G. D. Hallewell[103], J. A. Hallford[48], K. Hamano[170], H. Hamdaoui[166], M. Hamer[25], S. E. D. Hammoud[66], E. J. Hampshire[96], J. Han[142a], L. Han[113a], L. Han[62], S. Han[14], K. Hanagaki[83], M. Hance[138], D. A. Hangal[42], H. Hanif[147], M. D. Hank[130], J. B. Hansen[43], P. H. Hansen[43], T. Harenberg[176], S. Harkusha[178], M. L. Harris[104], Y. T. Harris[25], J. Harrison[13], P. F. Harrison[172], M. L. E. Hart[97], N. M. Hartman[111], N. M. Hartmann[110], R. Z. Hasan[96,136], Y. Hasegawa[145], F. Haslbeck[128], S. Hassan[17], R. Hauser[108], M. Haviernik[135], C. M. Hawkes[21], R. J. Hawkings[37], Y. Hayashi[158], D. Hayden[108], C. Hayes[107], R. L. Hayes[116], C. P. Hays[128], J. M. Hays[95], H. S. Hayward[93], M. He[14,113c], Y. He[48], Y. He[97], N. B. Heatley[95], V. Hedberg[99], J. Heilman[35], S. Heim[48], T. Heim[18a], J. J. Heinrich[125], L. Heinrich[111], J. Hejbal[133], M. Helbig[50], A. Held[175], S. Hellesund[17], C. M. Helling[169], S. Hellman[47a,47b], A. M. Henriques Correia[37], H. Herde[99], Y. Hernández Jiménez[150], L. M. Herrmann[25], T. Herrmann[50], G. Herten[54], R. Hertenberger[110], L. Hervas[37], M. E. Hesping[101], N. P. Hessey[161a], J. Hessler[111], M. Hidaoui[36b], N. Hidic[135], E. Hill[160], T. S. Hillersoy[17], S. J. Hillier[21], J. R. Hinds[108], F. Hinterkeuser[25], M. Hirose[126], S. Hirose[162], D. Hirschbuehl[176], T. G. Hitchings[102], B. Hiti[94], J. Hobbs[150], R. Hobincu[28e], N. Hod[174], A. M. Hodges[167], M. C. Hodgkinson[144], B. H. Hodkinson[128], A. Hoecker[37], D. D. Hofer[107], J. Hofer[168], J. Hofner[101], M. Holzbock[37], L. B. A. H. Hommels[33], V. Homsak[128], J. J. Hong[68], T. M. Hong[131], B. H. Hooberman[167], W. H. Hopkins[6], M. C. Hoppesch[167], Y. Horii[112], M. E. Horstmann[111], S. Hou[153], M. R. Housenga[167], J. Howarth[59], J. Hoya[6], M. Hrabovsky[124], T. Hryn'ova[4], P. J. Hsu[65], S.-C. Hsu[141], T. Hsu[66], M. Hu[18a], Q. Hu[62], S. Huang[33], X. Huang[14,113c], Y. Huang[135], Y. Huang[113b], Y. Huang[14], Z. Huang[66], Z. Hubacek[134], F. Huegging[25], T. B. Huffman[128], M. Hufnagel Maranha De Faria[82a], C. A. Hugli[48], M. Huhtinen[37], S. K. Huiberts[127], R. Hulsken[105], C. E. Hultquist[18a], D. L. Humphreys[104], N. Huseynov[12], J. Huston[108], B. Huth[37], J. Huth[61], L. Huth[48], R. Hyneman[7], G. Iacobucci[56], G. Iakovidis[30], L. Iconomidou-Fayard[66], J. P. Iddon[37], P. Iengo[72a,72b], Y. Iiyama[158], T. Iizawa[158], Y. Ikegami[83], D. Iliadis[157], N. Ilic[160], H. Imam[36a], G. Inacio Goncalves[82d], S. A. Infante Cabanas[139c], T. Ingebretsen Carlson[47a,47b], J. M. Inglis[95], G. Introzzi[73a,73b], M. Iodice[77a], V. Ippolito[75a,75b], R. K. Irwin[93], M. Ishino[158], W. Islam[175], C. Issever[19], S. Istin[22a,ao], K. Itabashi[126], H. Ito[173], R. Iuppa[78a,78b], A. Ivina[174], S. Izumiyama[112], V. Izzo[72a], P. Jacka[134], P. Jackson[1], P. Jain[48], K. Jakobs[54], T. Jakoubek[174], J. Jamieson[59], W. Jang[158], S. Jankovych[135], M. Javurkova[104], P. Jawahar[102], L. Jeanty[125], J. Jejelava[154a,ae], P. Jenni[54,f], C. E. Jessiman[35], C. Jia[142a], H. Jia[169], J. Jia[150], X. Jia[111,113c], Z. Jia[113a], C. Jiang[52], Q. Jiang[64b], S. Jiggins[48], M. Jimenez Ortega[168], J. Jimenez Pena[13], S. Jin[113a], A. Jinaru[28b], O. Jinnouchi[140], P. Johansson[144], K. A. Johns[7], J. W. Johnson[138], F. A. Jolly[48], D. M. Jones[151], E. Jones[48], K. S. Jones[8], P. Jones[33], R. W. L. Jones[92], T. J. Jones[93], H. L. Joos[55], R. Joshi[121], J. Jovicevic[16], X. Ju[18a], J. J. Junggeburth[37], T. Junkermann[63a], A. Juste Rozas[13,x], M. K. Juzek[87], S. Kabana[139f], A. Kaczmarska[87], S. A. Kadir[148], M. Kado[111], H. Kagan[121], M. Kagan[148], A. Kahn[130], C. Kahra[101], T. Kaji[158], E. Kajomovitz[155], N. Kakati[174], N. Kakoty[13], I. Kalaitzidou[54], S. Kandel[8], N. Kanellos[10], N. J. Kang[138], D. Kar[34j], E. Karentzos[25], K. Karki[8], O. Karkout[116], S. N. Karpov[39], Z. M. Karpova[39], V. Kartvelishvili[92,154b], A. N. Karyukhin[38], E. Kasimi[157], J. Katzy[48], S. Kaur[35], K. Kawade[145], M. P. Kawale[122], C. Kawamoto[88], T. Kawamoto[62], E. F. Kay[37], S. Kazakos[108], V. F. Kazanin[38], J. M. Keaveney[34a], R. Keeler[170], G. V. Kehris[61], J. S. Keller[35], J. M. Kelly[170], J. J. Kempster[151], O. Kepka[133], J. Kerr[161b], B. P. Kerridge[136], B. P. Kerševan[94], L. Keszeghova[29a], R. A. Khan[131], A. Khanov[123], A. G. Kharlamov[38], T. Kharlamova[38], E. E. Khoda[141], M. Kholodenko[132a], T. J. Khoo[19], G. Khoriauli[171], Y. Khoulaki[36a], Y. A. R. Khwaira[129], B. Kibirige[34j], D. Kim[6], D. W. Kim[18b], Y. K. Kim[40], N. Kimura[97], M. K. Kingston[55], A. Kirchhoff[55], C. Kirfel[25], F. Kirfel[25], J. Kirk[136], A. E. Kiryunin[111], S. Kita[162], O. Kivernyk[25], M. Klassen[163], C. Klein[35], L. Klein[171], M. H. Klein[45], S. B. Klein[56], U. Klein[93], A. Klimentov[30], T. Klioutchnikova[37], P. Kluit[116], S. Kluth[111], E. Kneringer[79], T. M. Knight[160], A. Knue[49], M. Kobel[50], D. Kobylianskii[174], S. F. Koch[128], M. Kocian[148], P. Kodyš[135], D. M. Koeck[125], T. Koffas[35], O. Kolay[50], I. Koletsou[4], T. Komarek[87], K. Köneke[55], A. X. Y. Kong[1], T. Kono[120], N. Konstantinidis[97], P. Kontaxakis[56], B. Konya[99], R. Kopeliansky[42], S. Koperny[86a], R. Koppenhofer[54],

K. Korcyl[87], K. Kordas[157,d], A. Korn[97], S. Korn[55], I. Korolkov[13], N. Korotkova[38], B. Kortman[116], O. Kortner[111], S. Kortner[111], W. H. Kostecka[117], M. Kostov[29a], V. V. Kostyukhin[146], A. Kotsokechagia[37], A. Kotwal[51], A. Koulouris[37], A. Kourkoumeli-Charalampidi[73a,73b], C. Kourkoumelis[9], E. Kourlitis[111], O. Kovanda[125], R. Kowalewski[170], W. Kozanecki[125], A. S. Kozhin[38], V. A. Kramarenko[38], G. Kramberger[94], P. Kramer[25], M. W. Krasny[129], A. Krasznahorkay[104], A. C. Kraus[117], J. W. Kraus[176], J. A. Kremer[48], N. B. Krengel[146], T. Kresse[50], L. Kretschmann[176], J. Kretzschmar[93], P. Krieger[160], K. Krizka[21], K. Kroeninger[49], H. Kroha[111], J. Kroll[133], J. Kroll[130], K. S. Krowpman[108], U. Kruchonak[39], H. Krüger[25], N. Krumnack[80], M. C. Kruse[51], O. Kuchinskaia[39], S. Kuday[3a], S. Kuehn[37], R. Kuesters[54], T. Kuhl[48], V. Kukhtin[39], Y. Kulchitsky[39], S. Kuleshov[139b,139d], J. Kull[1], E. V. Kumar[110], M. Kumar[34j], N. Kumari[48], P. Kumari[161b], A. Kupco[133], A. Kupich[38], O. Kuprash[54], H. Kurashige[85], L. L. Kurchaninov[161a], O. Kurdysh[4], A. Kurova[38], M. Kuze[140], A. K. Kvam[104], J. Kvita[124], N. G. Kyriacou[141], M. Laassiri[30], C. Lacasta[168], F. Lacava[75a,75b], H. Lacker[19], D. Lacour[129], N. N. Lad[97], E. Ladygin[39], A. Lafarge[41], B. Laforge[129], T. Lagouri[177], F. Z. Lahbabi[36a], S. Lai[37,55], W. S. Lai[97], I. K. Lakomiec[55], J. E. Lambert[170], S. Lammers[68], W. Lampl[7], C. Lampoudis[157,d], G. Lamprinoudis[171], A. N. Lancaster[117], E. Lançon[30], U. Landgraf[54], M. P. J. Landon[95], V. S. Lang[54], A. J. Lankford[164], F. Lanni[37], C. S. Lantz[167], K. Lantzsch[25], A. Lanza[73a], M. Lanzac Berrocal[168], J. F. Laporte[137], T. Lari[71a], D. Larsen[17], L. Larson[11], F. Lasagni Manghi[24b], M. Lassnig[37], S. D. Lawlor[144], R. Lazaridou[164], M. Lazzaroni[71a,71b], E. T. T. Le[164], H. D. M. Le[108], E. M. Le Boulicaut[177], L. T. Le Pottier[18a], B. Leban[24a,24b], F. Ledroit-Guillon[60], T. F. Lee[161b], L. L. Leeuw[34c], M. Lefebvre[170], C. Leggett[18a], G. Lehmann Miotto[37], M. Leigh[56], W. A. Leight[104], W. Leinonen[115], A. Leisos[157,u], M. A. L. Leite[82c], C. E. Leitgeb[19], R. Leitner[135], K. J. C. Leney[45], T. Lenz[25], S. Leone[74a], C. Leonidopoulos[52], A. Leopold[149], J. LePage Bourbonnais[35], R. Les[108], C. G. Lester[33], M. Levchenko[38], J. Levêque[4], L. J. Levinson[174], G. Levrini[24a,24b], M. P. Lewicki[87], C. Lewis[141], D. J. Lewis[4], L. Lewitt[144], A. Li[30], B. Li[142a], C. Li[107], C.-Q. Li[111], H. Li[142a], H. Li[102], H. Li[15], H. Li[62], H. Li[142a], J. Li[143a], K. Li[14], L. Li[143a], R. Li[177], S. Li[14,113c], S. Li[143a,143b], T. Li[5], X. Li[105], Y. Li[14], Z. Li[158], Z. Li[14,113c], Z. Li[62], S. Liang[14,113c], Z. Liang[14], M. Liberatore[137], B. Liberti[76a], G. B. Libotte[82d], K. Lie[64c], J. Lieber Marin[82e], H. Lien[68], H. Lin[107], S. F. Lin[150], L. Linden[110], R. E. Lindley[7], J. H. Lindon[37], J. Ling[61], E. Lipeles[130], A. Lipniacka[17], A. Lister[169], J. D. Little[68], B. Liu[14], B. X. Liu[113b], D. Liu[155], D. Liu[138], E. H. L. Liu[21], J. K. K. Liu[119], K. Liu[143b], K. Liu[143a,143b], M. Liu[62], M. Y. Liu[62], P. Liu[14], Q. Liu[148], S. Liu[150], X. Liu[142a], Y. Liu[113b,113c], Y. Liu[167], Y. L. Liu[142a], Y. W. Liu[62], Z. Liu[66,k], S. L. Lloyd[95], E. M. Lobodzinska[48], P. Loch[7], E. Lodhi[160], K. Lohwasser[144], E. Loiacono[48], J. D. Lomas[21], J. D. Long[42], I. Longarini[164], R. Longo[167], A. Lopez Solis[13], N. A. Lopez-canelas[7], N. Lorenzo Martinez[4], A. M. Lory[110], M. Losada[118a], G. Löschcke Centeno[4], X. Lou[47a,47b], X. Lou[14,113c], A. Lounis[66], P. A. Love[92], M. Lu[66], S. Lu[130], Y. J. Lu[153], H. J. Lubatti[141], C. Luci[75a,75b], F. L. Lucio Alves[113a], F. Luehring[68], B. S. Lunday[130], O. Lundberg[149], J. Lunde[37], N. A. Luongo[6], M. S. Lutz[37], A. B. Lux[26], D. Lynn[30], R. Lysak[133], V. Lysenko[134], E. Lytken[99], V. Lyubushkin[39], T. Lyubushkina[39], M. M. Lyukova[150], H. Ma[30], K. Ma[62], L. L. Ma[142a], W. Ma[62], Y. Ma[123], J. C. MacDonald[101], P. C. Machado De Abreu Farias[82e], D. Macina[37], R. Madar[41], T. Madula[97], J. Maeda[85], T. Maeno[30], P. T. Mafa[34c,j], H. Maguire[144], M. Maheshwari[33], V. Maiboroda[66], A. Maio[132a,132b,132d], K. Maj[86a], O. Majersky[48], S. Majewski[125], R. Makhmanazarov[38], N. Makovec[66], V. Maksimovic[16], B. Malaescu[129], J. Malamant[127], Pa. Malecki[87], V. P. Maleev[38], F. Malek[60,o], M. Mali[94], D. Malito[96], A. Maloizel[5], S. Maltezos[10], A. Malvezzi Lopes[82d], S. Malyukov[39], J. Mamuzic[94], G. Mancini[53], M. N. Mancini[27], G. Manco[73a,73b], J. P. Mandalia[95], S. S. Mandarry[151], I. Mandić[94], L. Manhaes de Andrade Filho[82a], I. M. Maniatis[174], J. Manjarres Ramos[90], D. C. Mankad[174], A. Mann[110], T. Manoussos[37], M. N. Mantinan[40], S. Manzoni[37], L. Mao[143a], X. Mapekula[34c], A. Marantis[157], R. R. Marcelo Gregorio[95], G. Marchiori[5], C. Marcon[71a], E. Maricic[16], M. Marinescu[48], S. Marium[48], M. Marjanovic[122], A. Markhoos[54], M. Markovitch[66], M. K. Maroun[104], M. C. Marr[147], G. T. Marsden[102], E. J. Marshall[92], Z. Marshall[18a], S. Marti-Garcia[168], J. Martin[97], T. A. Martin[136], V. J. Martin[52], B. Martin dit Latour[17], L. Martinelli[75a,75b], M. Martinez[13,x], P. Martinez Agullo[168], V. I. Martinez Outschoorn[104], P. Martinez Suarez[37], S. Martin-Haugh[136], G. Martinovicova[135], V. S. Martoiu[28b], A. C. Martyniuk[97], A. Marzin[37], D. Mascione[78a,78b], L. Masetti[101], J. Masik[102], A. L. Maslennikov[39], S. L. Mason[42], P. Massarotti[72a,72b], P. Mastrandrea[74a,74b], A. Mastroberardino[44a,44b], T. Masubuchi[126], T. T. Mathew[125], J. Matousek[135], D. M. Mattern[49], K. Mauer[48], J. Maurer[28b], T. Maurin[59], A. J. Maury[66], B. Maček[94], C. Mavungu Tsava[103], D. A. Maximov[38], A. E. May[102], E. Mayer[41],

R. Mazini[34j], I. Maznas[117], S. M. Mazza[138], E. Mazzeo[37], J. P. Mc Gowan[170], S. P. Mc Kee[107], C. A. Mc Lean[6], C. C. McCracken[169], E. F. McDonald[106], A. E. McDougall[116], L. F. Mcelhinney[92], J. A. Mcfayden[151], R. P. McGovern[130], R. P. Mckenzie[34j], T. C. Mclachlan[48], D. J. Mclaughlin[97], S. J. McMahon[136], C. M. Mcpartland[93], R. A. McPherson[170,ab], S. Mehlhase[110], A. Mehta[93], D. Melini[168], B. R. Mellado Garcia[34j], A. H. Melo[55], F. Meloni[48], A. M. Mendes Jacques Da Costa[102], L. Meng[92], S. Menke[111], M. Mentink[37], E. Meoni[44a,44b], G. Mercado[117], S. Merianos[157], C. Merlassino[69a,69c], C. Meroni[71a,71b], J. Metcalfe[6], A. S. Mete[6], E. Meuser[101], C. Meyer[68], J.-P. Meyer[137], Y. Miao[113a], R. P. Middleton[136], M. Mihovilovic[66], L. Mijović[52], G. Mikenberg[174], M. Mikestikova[133], M. Mikuž[94], H. Mildner[101], A. Milic[37], D. W. Miller[40], E. H. Miller[148], A. Milov[174], D. A. Milstead[47a,47b], T. Min[113a], A. A. Minaenko[38], I. A. Minashvili[154b], A. I. Mincer[119], B. Mindur[86a], M. Mineev[39], Y. Mino[88], L. M. Mir[13], M. Miralles Lopez[59], M. Mironova[18a], M. Missio[41], A. Mitra[172], V. A. Mitsou[168], Y. Mitsumori[112], O. Miu[160], P. S. Miyagawa[95], T. Mkrtchyan[37], M. Mlinarevic[97], T. Mlinarevic[97], M. Mlynarikova[135], L. Mlynarska[86a], C. Mo[143a], S. Mobius[20], M. H. Mohamed Farook[114], S. Mohapatra[42], M. F. Mohd Soberi[52], S. Mohiuddin[123], G. Mokgatitswane[34j], L. Moleri[174], U. Molinatti[128], L. G. Mollier[20], B. Mondal[133], S. Mondal[134], K. Mönig[48], E. Monnier[103], L. Monsonis Romero[168], J. Montejo Berlingen[13], A. Montella[47a,47b], M. Montella[121], F. Montereali[77a,77b], F. Monticelli[91], S. Monzani[69a,69c], A. Morancho Tarda[43], N. Morange[66], A. L. Moreira De Carvalho[48], M. Moreno Llácer[168], C. Moreno Martinez[56], J. M. Moreno Perez[23b], P. Morettini[57b], S. Morgenstern[37], M. Morii[61], M. Morinaga[158], M. Moritsu[89], F. Morodei[75a,75b], P. Moschovakos[37], B. Moser[54], M. Mosidze[154b], T. Moskalets[45], P. Moskvitina[115], J. Moss[32], P. Moszkowicz[86a], T. Motta Quirino[82d], A. Moussa[36d], Y. Moyal[174], H. Moyano Gomez[13], E. J. W. Moyse[104], T. G. Mroz[87], S. Muanza[103], M. Mucha[25], J. Mueller[131], G. A. Mullier[166], A. J. Mullin[33], J. J. Mullin[51], A. C. Mullins[45], A. E. Mulski[61], D. P. Mungo[160], D. Munoz Perez[168], F. J. Munoz Sanchez[102], W. J. Murray[136,172], M. Muškinja[94], C. Mwewa[48], A. G. Myagkov[38,a], A. J. Myers[8], G. Myers[107], M. Myska[134], B. P. Nachman[148], K. Nagai[128], K. Nagano[83], R. Nagasaka[158], J. L. Nagle[30,al], E. Nagy[103], A. M. Nairz[37], Y. Nakahama[83], K. Nakamura[83], K. Nakkalil[5], A. Nandi[63b], H. Nanjo[126], E. A. Narayanan[45], Y. Narukawa[158], I. Naryshkin[38], L. Nasella[71a,71b], S. Nasri[118b], C. Nass[25], G. Navarro[23a], A. Nayaz[19], P. Y. Nechaeva[38], S. Nechaeva[24a,24b], F. Nechansky[133], L. Nedic[128], T. J. Neep[21], A. Negri[73a,73b], M. Negrini[24b], C. Nellist[116], C. Nelson[105], K. Nelson[107], S. Nemecek[133], M. Nessi[37,g], M. S. Neubauer[167], J. Newell[93], P. R. Newman[21], Y. W. Y. Ng[167], B. Ngair[118a], H. D. N. Nguyen[109], J. D. Nichols[122], R. B. Nickerson[128], R. Nicolaidou[137], J. Nielsen[138], M. Niemeyer[55], J. Niermann[37], N. Nikiforou[37], V. Nikolaenko[38,a], I. Nikolic-Audit[129], P. Nilsson[30], I. Ninca[48], G. Ninio[156], A. Nisati[75a], R. Nisius[111], N. Nitika[174], E. K. Nkadimeng[34b], T. Nobe[158], D. Noll[148], T. Nommensen[152], M. B. Norfolk[144], B. J. Norman[35], L. C. Nosler[18a], M. Noury[36a], J. Novak[94], T. Novak[94], P. Novotny[174], R. Novotny[134], L. Nozka[124], K. Ntekas[164], D. Ntounis[148], N. M. J. Nunes De Moura Junior[82b], J. Ocariz[129], I. Ochoa[132a], A. Odella Rodriguez[13], S. Oerdek[48,y], J. T. Offermann[40], A. Ogrodnik[87], A. Oh[102], C. C. Ohm[149], H. Oide[83], M. L. Ojeda[37], Y. Okumura[158], L. F. Oleiro Seabra[132a], I. Oleksiyuk[56], G. Oliveira Correa[13], D. Oliveira Damazio[30], J. L. Oliver[1], R. Omar[68], Ö. O. Öncel[54], A. P. O'Neill[20], Y. Onoda[140], A. Onofre[132a,132e,e], P. U. E. Onyisi[11], M.J. Oreglia[40], D. Orestano[77a,77b], R. Orlandini[77a,77b], R. S. Orr[160], L. M. Osojnak[42], Y. Osumi[112], G. Otero y Garzon[31], H. Otono[89], M. Ouchrif[36d], F. Ould-Saada[127], T. Ovsiannikova[141], M. Owen[59], R. E. Owen[136], V. E. Ozcan[22a], F. Ozturk[87], N. Ozturk[8], S. Ozturk[81], H. A. Pacey[128], K. Pachal[161a], A. Pacheco Pages[13], C. Padilla Aranda[13], G. Padovano[75a,75b], S. Pagan Griso[18a], J. Pampel[25], J. Pan[177], D. K. Panchal[11], C. E. Pandini[60], J. G. Panduro Vazquez[136], H. D. Pandya[1], H. Pang[137], P. Pani[48], G. Panizzo[69a,69c], L. Panwar[129], L. Paolozzi[56], S. Parajuli[167], A. Paramonov[6], C. Paraskevopoulos[53], D. Paredes Hernandez[64b], S. R. Paredes Saenz[52], A. Pareti[73a,73b], K. R. Park[42], T. H. Park[111], F. Parodi[57a,57b], J. A. Parsons[42], U. Parzefall[54], B. Pascual Dias[41], L. Pascual Dominguez[100], E. Pasqualucci[75a], S. Passaggio[57b], F. Pastore[96], P. Patel[87], U. M. Patel[51], J. R. Pater[102], T. Pauly[37], F. Pauwels[135], C. I. Pazos[163], M. Pedersen[127], R. Pedro[132a], S. V. Peleganchuk[38], O. Penc[133], S. Peng[15], G. D. Penn[177], K. E. Penski[110], M. Penzin[38], B. S. Peralva[82d], A. P. Pereira Peixoto[141], L. Pereira Sanchez[148], D. V. Perepelitsa[30,al], G. Perera[104], E. Perez Codina[37], M. Perganti[10], H. Pernegger[37], S. Perrella[75a,75b], K. Peters[48], R. F. Y. Peters[102], B. A. Petersen[37], T. C. Petersen[43], E. Petit[103], V. Petousis[134], A. R. Petri[71a,71b], C. Petridou[157,d], T. Petru[135], M. Pettee[18a], A. Petukhov[81], K. Petukhova[37], R. Pezoa[139g], L. Pezzotti[24a,24b], G. Pezzullo[177], L. Pfaffenbichler[37], A. J. Pfleger[79], T. M. Pham[175], T. Pham[106], P. W. Phillips[136], G. Piacquadio[150],

E. Pianori[18a], F. Piazza[125], R. Piegaia[31], D. Pietreanu[28b], A. D. Pilkington[102], M. Pinamonti[69a,69c], J. L. Pinfold[2], G. Pinheiro Matos[42], B. C. Pinheiro Pereira[132a], J. Pinol Bel[13], A. E. Pinto Pinoargote[129], L. Pintucci[69a,69c], K. M. Piper[151], A. Pirttikoski[56], D. A. Pizzi[35], L. Pizzimento[64b], A. Plebani[33], M.-A. Pleier[30], V. Pleskot[135], E. Plotnikova[39], G. Poddar[95], R. Poettgen[99], L. Poggioli[129], S. Polacek[135], G. Polesello[73a], A. Poley[147], A. Polini[24b], C. S. Pollard[172], Z. B. Pollock[121], E. Pompa Pacchi[122], N. I. Pond[97], D. Ponomarenko[68], L. Pontecorvo[37], S. Popa[28a], G. A. Popeneciu[28d], A. Poreba[37], D. M. Portillo Quintero[161a], S. Pospisil[134], M. A. Postill[144], P. Postolache[28c], K. Potamianos[172], P. A. Potepa[86a], I. N. Potrap[39], C. J. Potter[33], H. Potti[152], J. Poveda[168], M. E. Pozo Astigarraga[37], R. Pozzi[37], A. Prades Ibanez[76a,76b], S. R. Pradhan[144], J. Pretel[170], D. Price[102], M. Primavera[70a], L. Primomo[69a,69c], M. A. Principe Martin[100], R. Privara[124], T. Procter[86b], M. L. Proffitt[141], N. Proklova[130], K. Prokofiev[64c], G. Proto[111], J. Proudfoot[6], M. Przybycien[86a], W. W. Przygoda[86b], A. Psallidas[46], J. E. Puddefoot[144], D. Pudzha[53], H. I. Purnell[1], D. Pyatiizbyantseva[115], J. Qian[107], R. Qian[108], D. Qichen[128], Y. Qin[13], T. Qiu[52], A. Quadt[55], M. Queitsch-Maitland[102], G. Quetant[56], R. P. Quinn[169], G. Rabanal Bolanos[61], D. Rafanoharana[111], F. Raffaeli[76a,76b], F. Ragusa[71a,71b], J. L. Rainbolt[40], S. Rajagopalan[30], E. Ramakoti[39], L. Rambelli[57a,57b], I. A. Ramirez-Berend[35], K. Ran[107,113c], D. S. Rankin[130], N. P. Rapheeha[34j], H. Rasheed[28b], A. Rastogi[18a], S. Rave[101], S. Ravera[57a,57b], B. Ravina[37], I. Ravinovich[174], M. Raymond[37], A. L. Read[127], N. P. Readioff[144], D. M. Rebuzzi[73a,73b], A. S. Reed[59], K. Reeves[27], D. Reikher[37], A. Rej[49], C. Rembser[37], H. Ren[62], M. Renda[28b], F. Renner[48], A. G. Rennie[59], M. Repik[56], A. L. Rescia[57a,57b], S. Resconi[71a], M. Ressegotti[57a,57b], S. Rettie[116], W. F. Rettie[35], M. M. Revering[33], E. Reynolds[18a], O. L. Rezanova[39], P. Reznicek[135], H. Riani[36d], N. Ribaric[51], B. Ricci[69a,69c], E. Ricci[78a,78b], R. Richter[111], S. Richter[47a,47b], E. Richter-Was[86b], M. Ridel[129], S. Ridouani[36d], P. Rieck[119], P. Riedler[37], E. M. Riefel[47a,47b], J. O. Rieger[116], M. Rijssenbeek[150], M. Rimoldi[34c], L. Rinaldi[24a,24b], P. Rincke[55,166], G. Ripellino[166], I. Riu[13], J. C. Rivera Vergara[170], F. Rizatdinova[123], E. Rizvi[95], B. R. Roberts[40], S. S. Roberts[138], D. Robinson[33], A. Robson[59], A. Rocchi[76a,76b], C. Roda[74a,74b], F. A. Rodriguez[117], S. Rodriguez Bosca[37], Y. Rodriguez Garcia[23a], A. M. Rodríguez Vera[117], S. Roe[37], J. T. Roemer[37], O. Røhne[127], R. A. Rojas[37], C. P. A. Roland[129], A. Romaniouk[79], E. Romano[73a,73b], M. Romano[24b], A. C. Romero Hernandez[167], N. Rompotis[93], L. Roos[129], S. Rosati[75a], B. J. Rosser[40], E. Rossi[128], E. Rossi[72a,72b], L. P. Rossi[61], L. Rossini[54], R. Rosten[121], M. Rotaru[28b], R. Roth[37], D. Rousseau[66], D. Rousso[48], S. Roy-Garand[160], A. Rozanov[103], Z. M. A. Rozario[59], Y. Rozen[155], A. Rubio Jimenez[168], V. H. Ruelas Rivera[19], T. A. Ruggeri[1], A. Ruggiero[128], A. Ruiz-Martinez[168], A. Rummler[37], G. B. Rupnik Boero[37], Z. Rurikova[54], N. A. Rusakovich[39], S. Ruscelli[49], H. L. Russell[170], G. Russo[75a,75b], J. P. Rutherfoord[7], S. Rutherford Colmenares[33], M. Rybar[135], P. Rybczynski[86a], A. Ryzhov[45], H. F.-W. Sadrozinski[138], F. Safai Tehrani[75a], S. Saha[1], M. Sahinsoy[81], B. Sahoo[174], A. Saibel[168], B. T. Saifuddin[122], M. Saimpert[137], G. T. Saito[82c], M. Saito[158], T. Saito[158], A. Sala[71a,71b], A. Salnikov[148], J. Salt[168], A. Salvador Salas[156], F. Salvatore[151], A. Salzburger[37], D. Sammel[54], E. Sampson[92], D. Sampsonidis[157,d], D. Sampsonidou[125], M. A. A. Samy[59], J. Sánchez[168], V. Sanchez Sebastian[168], H. Sandaker[127], C. O. Sander[48], J. A. Sandesara[175], M. Sandhoff[176], C. Sandoval[23b], L. Sanfilippo[63a], D. P. C. Sankey[136], T. Sano[88], A. Sansoni[53], M. Santana Queiroz[18b], L. Santi[37], C. Santoni[41], H. Santos[132a,132b], A. Santra[174], E. Sanzani[24a,24b], K. A. Saoucha[84b], J. G. Saraiva[132a,132d], J. Sardain[7], O. Sasaki[83], K. Sato[162], C. Sauer[37], E. Sauvan[4], P. Savard[160,ai], R. Sawada[158], C. Sawyer[136], L. Sawyer[98], A. M. Sayed[27], C. Sbarra[24b], A. Sbrizzi[24a,24b], T. Scanlon[97], J. Schaarschmidt[141], U. Schäfer[101], A. C. Schaffer[45,66], D. Schaile[110], R. D. Schamberger[150], C. Scharf[19], M. M. Schefer[20], V. A. Schegelsky[38], D. Scheirich[135], M. Schernau[139f], C. Scheulen[56], C. Schiavi[57a,57b], M. Schioppa[44a,44b], B. Schlag[148], S. Schlenker[37], J. Schmeing[176], E. Schmidt[111], M. A. Schmidt[176], K. Schmieden[25], C. Schmitt[101], N. Schmitt[101], S. Schmitt[48], N. A. Schneider[110], L. Schoeffel[137], A. Schoening[63b], P. G. Scholer[35], E. Schopf[146], M. Schott[25], S. Schramm[56], T. Schroer[56], H.-C. Schultz-Coulon[63a], M. Schumacher[54], B. A. Schumm[138], Ph. Schune[137], H. R. Schwartz[7], A. Schwartzman[148], T. A. Schwarz[107], Ph. Schwemling[137], R. Schwienhorst[108], F. G. Sciacca[20], A. Sciandra[30], G. Sciolla[27], F. Scuri[74a], C. D. Sebastiani[37], K. Sedlaczek[117], S. C. Seidel[114], A. Seiden[138], B. D. Seidlitz[42], C. Seitz[48], J. M. Seixas[82b], G. Sekhniaidze[72a], L. Selem[60], N. Semprini-Cesari[24a,24b], A. Semushin[178], D. Sengupta[56], V. Senthilkumar[168], L. Serin[66], M. Sessa[72a,72b], H. Severini[122], F. Sforza[57a,57b], A. Sfyrla[56], Q. Sha[14], H. Shaddix[117], A. H. Shah[33], R. Shaheen[149], J. D. Shahinian[130], M. Shamim[37], L. Y. Shan[14], M. Shapiro[18a], A. Sharma[37], A. S. Sharma[169], P. Sharma[30], P. B. Shatalov[38], K. Shaw[151], S. M. Shaw[102],

Q. Shen[14], D. J. Sheppard[147], P. Sherwood[97], L. Shi[97], X. Shi[14], S. Shimizu[83], I. P. J. Shipsey[128,*], S. Shirabe[89], M. Shiyakova[39,z], M. J. Shochet[40], D. R. Shope[127], B. Shrestha[122], S. Shrestha[121,an], I. Shreyber[39], M. J. Shroff[170], P. Sicho[133], A. M. Sickles[167], E. Sideras Haddad[34j,165], A. C. Sidley[116], A. Sidoti[24b], F. Siegert[50], Dj. Sijacki[16], F. Sili[62], J. M. Silva[52], I. Silva Ferreira[82b], M. V. Silva Oliveira[30], S. B. Silverstein[47a], S. Simion[66], R. Simoniello[37], E. L. Simpson[102], H. Simpson[151], L. R. Simpson[6], S. Simsek[81], S. Sindhu[55], S. N. Singh[27], S. Singh[30], S. Sinha[48], S. Sinha[102], M. Sioli[24a,24b], K. Sioulas[9], I. Siral[37], E. Sitnikova[48], J. Sjölin[47a,47b], A. Skaf[55], E. Skorda[21], P. Skubic[122], M. Slawinska[87], I. Slazyk[17], I. Sliusar[127], V. Smakhtin[174], B. H. Smart[136], S. Yu. Smirnov[139b], Y. Smirnov[34c], L. N. Smirnova[38,a], O. Smirnova[99], A. C. Smith[42], D. R. Smith[164], J. L. Smith[102], M. B. Smith[35], R. Smith[148], H. Smitmanns[101], M. Smizanska[92], K. Smolek[134], P. Smolyanskiy[134], A. A. Snesarev[39], H. L. Snoek[116], R. M. Snyder[51], S. Snyder[30], R. Sobie[170,ab], A. Soffer[156], C. A. Solans Sanchez[37], E. Yu. Soldatov[39], U. Soldevila[168], A. A. Solodkov[34j], S. Solomon[27], A. Soloshenko[39], K. Solovieva[54], O. V. Solovyanov[41], P. Sommer[50], A. Sonay[13], A. Sopczak[134], A. L. Sopio[52], F. Sopkova[29b], J. D. Sorenson[114], I. R. Sotarriva Alvarez[140], V. Sothilingam[63a], O. J. Soto Sandoval[139b,139c], S. Sottocornola[68], R. Soualah[84a], Z. Soumaimi[36e], D. South[48], N. Soybelman[174], S. Spagnolo[70a,70b], D. Sperlich[54], B. Spisso[72a,72b], D. P. Spiteri[59], L. Splendori[103], M. Spousta[135], E. J. Staats[35], R. Stamen[63a], E. Stanecka[87], W. Stanek-Maslouska[48], M. V. Stange[50], B. Stanislaus[18a], M. M. Stanitzki[48], E. A. Starchenko[38], G. H. Stark[138], J. Stark[90], P. Staroba[133], P. Starovoitov[84b], R. Staszewski[87], C. Stauch[110], G. Stavropoulos[46], A. Stefl[37], A. Stein[101], P. Steinberg[30], B. Stelzer[147,161a], H. J. Stelzer[131], O. Stelzer[161a], H. Stenzel[58], T. J. Stevenson[151], G. A. Stewart[37], J. R. Stewart[123], G. Stoicea[28b], M. Stolarski[132a], S. Stonjek[111], A. Straessner[50], J. Strandberg[149], S. Strandberg[47a,47b], M. Stratmann[176], M. Strauss[122], T. Strebler[103], P. Strizenec[29b], R. Ströhmer[171], D. M. Strom[125], R. Stroynowski[45], A. Strubig[47a,47b], S. A. Stucci[30], B. Stugu[17], J. Stupak[122], N. A. Styles[48], D. Su[148], S. Su[62], X. Su[62], D. Suchy[29a], A. D. Sudhakar Ponnu[55], L. Sudit[174], K. Sugizaki[130], V. V. Sulin[38], D. M. S. Sultan[128], L. Sultanaliyeva[25], S. Sultansoy[3b], S. Sun[175], W. Sun[14], N. Sur[99], N. Suri Jr[177], M. R. Sutton[151], M. Svatos[133], P. N. Swallow[33], M. Swiatlowski[161a], A. Swoboda[37], I. Sykora[29a], M. Sykora[135], T. Sykora[135], D. Ta[101], K. Tackmann[48,y], A. Taffard[164], R. Tafirout[161a], Y. Takubo[83], M. Talby[103], A. A. Talyshev[38], K. C. Tam[64b], N. M. Tamir[156], A. Tanaka[158], J. Tanaka[158], R. Tanaka[66], M. Tanasini[150], Z. Tao[169], S. Tapia Araya[139g], S. Tapprogge[101], A. Tarek Abouelfadl Mohamed[37], S. Tarem[155], K. Tariq[14], G. Tarna[37], G. F. Tartarelli[71a], M. J. Tartarin[90], P. Tas[135], M. Tasevsky[133], E. Tassi[44a,44b], A. C. Tate[167], Y. Tayalati[36e,aa], G. N. Taylor[106], W. Taylor[161b], R. J. Taylor Vara[168], A. S. Tegetmeier[90], P. Teixeira-Dias[96], J. J. Teoh[160], K. Terashi[158], J. Terron[100], S. Terzo[13], M. Testa[53], R. J. Teuscher[160,ab], A. Thaler[79], O. Theiner[56], T. Theveneaux-Pelzer[103], D. W. Thomas[96], J. P. Thomas[21], E. A. Thompson[18a], P. D. Thompson[21], E. Thomson[130], R. E. Thornberry[45], C. Tian[62], Y. Tian[56], V. Tikhomirov[81], Yu. A. Tikhonov[39], S. Timoshenko[38], D. Timoshyn[135], E. X. L. Ting[1], P. Tipton[177], A. Tishelman-Charny[30], K. Todome[140], S. Todorova-Nova[135], L. Toffolin[69a,69c], M. Togawa[83], J. Tojo[89], S. Tokár[29a], O. Toldaiev[68], G. Tolkachev[103], M. Tomoto[83], L. Tompkins[148,n], E. Torrence[125], H. Torres[90], D. I. Torres Arza[139g], E. Torró Pastor[168], M. Toscani[31], C. Tosciri[40], M. Tost[11], D. R. Tovey[144], T. Trefzger[171], P. M. Tricarico[13], A. Tricoli[30], I. M. Trigger[161a], S. Trincaz-Duvoid[129], D. A. Trischuk[170], A. Tropina[39], D. Truncali[76a,76b], L. Truong[34c], M. Trzebinski[87], A. Trzupek[87], F. Tsai[150], M. Tsai[107], A. Tsiamis[157], P. V. Tsiareshka[39], S. Tsigaridas[161a], A. Tsirigotis[157,u], V. Tsiskaridze[154a], E. G. Tskhadadze[154a], Y. Tsujikawa[88], I. I. Tsukerman[38], V. Tsulaia[18a], S. Tsuno[83], K. Tsuri[120], D. Tsybychev[150], Y. Tu[64b], A. Tudorache[28b], V. Tudorache[28b], S. B. Tuncay[128], S. Turchikhin[57a,57b], I. Turk Cakir[3a], R. Turra[71a], T. Turtuvshin[39,ac], P. M. Tuts[42], S. Tzamarias[157,d], Y. Uematsu[83], F. Ukegawa[162], P. A. Ulloa Poblete[139b,139c], E. N. Umaka[30], G. Unal[37], A. Undrus[30], G. Unel[164], J. Urban[29b], P. Urrejola[139e], G. Usai[8], R. Ushioda[159], M. Usman[109], F. Ustuner[52], Z. Uysal[81], V. Vacek[134], B. Vachon[105], T. Vafeiadis[37], A. Vaitkus[97], C. Valderanis[110], E. Valdes Santurio[47a,47b], M. Valente[37], S. Valentinetti[24a,24b], A. Valero[168], E. Valiente Moreno[168], A. Vallier[90], J. A. Valls Ferrer[168], D. R. Van Arneman[116], A. Van Der Graaf[49], H. Z. Van Der Schyf[34j], P. Van Gemmeren[6], M. Van Rijnbach[37], S. Van Stroud[97], I. Van Vulpen[116], P. Vana[135], M. Vanadia[76a,76b], U. M. Vande Voorde[149], W. Vandelli[37], E. R. Vandewall[148], D. Vannicola[156], L. Vannoli[53], R. Vari[75a], M. Varma[177], E. W. Varnes[7], C. Varni[79], D. Varouchas[66], L. Varriale[168], K. E. Varvell[152], M. E. Vasile[28b], L. Vaslin[83], M. D. Vassilev[148], A. Vasyukov[39], L. M. Vaughan[123], R. Vavricka[135], T. Vazquez Schroeder[13], J. Veatch[32], V. Vecchio[102], M. J. Veen[104], I. Veliscek[30], I. Velkovska[94], L. M. Veloce[160], F. Veloso[132a,132c], A. G. Veltman[52], S. H. Venetianer[163], S. Veneziano[75a],

A. Ventura[70a,70b], A. Verbytskyi[111], M. Verducci[74a,74b], C. Vergis[95], M. Verissimo De Araujo[82b], W. Verkerke[116], J. C. Vermeulen[116], C. Vernieri[148], M. Vessella[164], M. C. Vetterli[147,ai], A. Vgenopoulos[101], N. Viaux Maira[139g,af], T. Vickey[144], O. E. Vickey Boeriu[144], G. H. A. Viehhauser[128], L. Vigani[63b], M. Vigl[111], M. Villa[24a,24b], M. Villaplana Perez[168], E. M. Villhauer[40], E. Vilucchi[53], M. Vincent[168], M. G. Vincter[35], A. Visibile[116], A. Visive[116], C. Vittori[37], I. Vivarelli[24a,24b], M. I. Vivas Albornoz[48], E. Voevodina[111], F. Vogel[110], J. C. Voigt[50], P. Vokac[134], Yu. Volkotrub[86b], L. Vomberg[25], E. Von Toerne[25], B. Vormwald[37], K. Vorobev[51], M. Vos[168], K. Voss[146], M. Vozak[37], L. Vozdecky[122], N. Vranjes[16], M. Vranjes Milosavljevic[16], M. Vreeswijk[116], N. K. Vu[143a,143b], R. Vuillermet[37], O. Vujinovic[101], I. Vukotic[40], I. K. Vyas[35], J. F. Wack[33], S. Wada[162], C. Wagner[148], J. M. Wagner[18a], W. Wagner[176], S. Wahdan[176], H. Wahlberg[91], C. H. Waits[122], J. Walder[136], R. Walker[110], K. Walkingshaw Pass[59], W. Walkowiak[146], A. Wall[130], E. J. Wallin[99], T. Wamorkar[148], K. Wandall-Christensen[168], A. Wang[62], A. Z. Wang[138], C. Wang[48], C. Wang[11], H. Wang[18a], J. Wang[64c], P. Wang[102], P. Wang[97], R. Wang[61], R. Wang[6], S. M. Wang[153], S. Wang[14], T. Wang[115], T. Wang[62], W. T. Wang[128], W. Wang[14], X. Wang[167], X. Wang[143a], X. Wang[48], Y. Wang[150], Y. Wang[114], Z. Wang[107], Z. Wang[143b], Z. Wang[107], C. Wanotayaroj[83], A. Warburton[105], A. L. Warnerbring[146], S. Waterhouse[96], A. T. Watson[21], H. Watson[52], M. F. Watson[21], E. Watton[37], G. Watts[141], B. M. Waugh[97], J. M. Webb[54], C. Weber[30], M. S. Weber[20], S. M. Weber[63a], C. Wei[62], Y. Wei[54], A. R. Weidberg[128], E. J. Weik[119], J. Weingarten[49], C. Weiser[54], C. J. Wells[48], T. Wenaus[30], T. Wengler[37], N. S. Wenke[111], N. Wermes[25], M. Wessels[63a], A. M. Wharton[92], A. S. White[61], A. White[8], M. J. White[1], D. Whiteson[164], L. Wickremasinghe[126], W. Wiedenmann[175], M. Wielers[136], R. Wierda[149], C. Wiglesworth[43], H. G. Wilkens[37], J. J. H. Wilkinson[33], D. M. Williams[42], H. H. Williams[130], S. Williams[33], S. Willocq[104], B. J. Wilson[102], D. J. Wilson[102], P. J. Windischhofer[40], F. I. Winkel[31], F. Winklmeier[125], B. T. Winter[54], M. Wittgen[148], M. Wobisch[98], T. Wojtkowski[60], Z. Wolffs[116], J. Wollrath[37], M. W. Wolter[87], H. Wolters[132a,132c], M. C. Wong[138], E. L. Woodward[42], S. D. Worm[48], B. K. Wosiek[87], K. W. Woźniak[87], S. Wozniewski[55], K. Wraight[59], C. Wu[160], C. Wu[21], J. Wu[158], M. Wu[113b], M. Wu[115], S. L. Wu[175], S. Wu[14,ak], X. Wu[62], Y. Q. Wu[160], Y. Wu[62], Z. Wu[4], Z. Wu[113a], J. Wuerzinger[111], T. R. Wyatt[102], B. M. Wynne[52], S. Xella[43], L. Xia[113a], M. Xie[62], A. Xiong[125], D. Xu[14], H. Xu[62], L. Xu[62], R. Xu[130], T. Xu[107], W. Xu[113a], Y. Xu[141], Z. Xu[52], R. Xue[131], B. Yabsley[152], S. Yacoob[34a], Y. Yamaguchi[83], E. Yamashita[158], H. Yamauchi[162], T. Yamazaki[18a], Y. Yamazaki[85], S. Yan[59], Z. Yan[104], H. J. Yang[143a,143b], H. T. Yang[62], S. Yang[62], T. Yang[64c], X. Yang[37], X. Yang[14], Y. Yang[158], Y. Yang[62], W.-M. Yao[18a], C. L. Yardley[151], J. Ye[14], S. Ye[30], X. Ye[62], Y. Yeh[97], I. Yeletskikh[39], B. Yeo[18b], M. R. Yexley[97], T. P. Yildirim[128], K. Yorita[173], C. J. S. Young[37], C. Young[148], I. N. L. Young[59], N. D. Young[125], Y. Yu[62], J. Yuan[14,113c,ak], M. Yuan[107], R. Yuan[143b], L. Yue[97], M. Zaazoua[62], B. Zabinski[87], I. Zahir[36a], A. Zaio[57a,57b], Z. K. Zak[87], T. Zakareishvili[168], S. Zambito[56], J. A. Zamora Saa[139d], J. Zang[158], R. Zanzottera[71a,71b], O. Zaplatilek[134], C. Zeitnitz[176], H. Zeng[14], D. T. Zenger Jr[27], O. Zenin[38], T. Ženiš[29a], S. Zenz[95], D. Zerwas[66], B. Zhang[172], D. F. Zhang[144], G. Zhang[14,ak], J. Zhang[142a], J. Zhang[6], L. Zhang[62], L. Zhang[113a], P. Zhang[14,113c], R. Zhang[113a], S. Zhang[90], T. Zhang[158], Y. Zhang[141], Y. Zhang[97], Y. Zhang[62], Y. Zhang[113a], Z. Zhang[18a], Z. Zhang[142a], Z. Zhang[66], H. Zhao[141], T. Zhao[142a], Y. Zhao[35], Z. Zhao[62], Z. Zhao[62], A. Zhemchugov[39], J. Zheng[113a], K. Zheng[167], X. Zheng[62], Z. Zheng[148], D. Zhong[167], B. Zhou[107], B. Zhou[143a,143b], H. Zhou[7], N. Zhou[143a], Y. Zhou[15], Y. Zhou[113a], Y. Zhou[7], J. Zhu[107], X. Zhu[143b], Y. Zhu[143a], Y. Zhu[62], X. Zhuang[14], K. Zhukov[68], N. I. Zimine[39], J. Zinsser[63b], M. Ziolkowski[146], L. Živković[16], A. Zoccoli[24a,24b], K. Zoch[61], A. Zografos[37], T. G. Zorbas[144], O. Zormpa[46], L. Zwalinski[37]

[1] Department of Physics, University of Adelaide, Adelaide, Australia
[2] Department of Physics, University of Alberta, Edmonton, AB, Canada
[3] [(a)]Department of Physics, Ankara University, Ankara, Türkiye; [(b)]Division of Physics, TOBB University of Economics and Technology, Ankara, Türkiye
[4] LAPP, Université Savoie Mont Blanc, CNRS/IN2P3, Annecy, France
[5] APC, Université Paris Cité, CNRS/IN2P3, Paris, France
[6] High Energy Physics Division, Argonne National Laboratory, Argonne, IL, USA
[7] Department of Physics, University of Arizona, Tucson, AZ, USA
[8] Department of Physics, University of Texas at Arlington, Arlington, TX, USA
[9] Physics Department, National and Kapodistrian University of Athens, Athens, Greece

[10] Physics Department, National Technical University of Athens, Zografou, Greece
[11] Department of Physics, University of Texas at Austin, Austin, TX, USA
[12] Institute of Physics, Azerbaijan Academy of Sciences, Baku, Azerbaijan
[13] Institut de Física d'Altes Energies (IFAE), Barcelona Institute of Science and Technology, Barcelona, Spain
[14] Institute of High Energy Physics, Chinese Academy of Sciences, Beijing, China
[15] Physics Department, Tsinghua University, Beijing, China
[16] Institute of Physics, University of Belgrade, Belgrade, Serbia
[17] Department for Physics and Technology, University of Bergen, Bergen, Norway
[18] [(a)]Physics Division, Lawrence Berkeley National Laboratory, Berkeley, CA, USA; [(b)]University of California, Berkeley, CA, USA
[19] Institut für Physik, Humboldt Universität zu Berlin, Berlin, Germany
[20] Albert Einstein Center for Fundamental Physics and Laboratory for High Energy Physics, University of Bern, Bern, Switzerland
[21] School of Physics and Astronomy, University of Birmingham, Birmingham, UK
[22] [(a)]Department of Physics, Bogazici University, Istanbul, Türkiye; [(b)]Department of Physics Engineering, Gaziantep University, Gaziantep, Türkiye; [(c)]Department of Physics, Istanbul University, Istanbul, Türkiye
[23] [(a)]Facultad de Ciencias y Centro de Investigaciónes, Universidad Antonio Nariño, Bogotá, Colombia; [(b)]Departamento de Física, Universidad Nacional de Colombia, Bogotá, Colombia
[24] [(a)]Dipartimento di Fisica e Astronomia A. Righi, Università di Bologna, Bologna, Italy; [(b)]INFN Sezione di Bologna, Bologna, Italy
[25] Physikalisches Institut, Universität Bonn, Bonn, Germany
[26] Department of Physics, Boston University, Boston, MA, USA
[27] Department of Physics, Brandeis University, Waltham, MA, USA
[28] [(a)]Transilvania University of Brasov, Brasov, Romania; [(b)]Horia Hulubei National Institute of Physics and Nuclear Engineering, Bucharest, Romania; [(c)]Department of Physics, Alexandru Ioan Cuza University of Iasi, Iasi , Romania; [(d)]National Institute for Research and Development of Isotopic and Molecular Technologies, Physics Department, Cluj-Napoca, Romania; [(e)]National University of Science and Technology Politechnica, Bucharest, Romania; [(f)]West University in Timisoara, Timisoara, Romania; [(g)]Faculty of Physics, University of Bucharest, Bucharest, Romania
[29] [(a)]Faculty of Mathematics, Physics and Informatics, Comenius University, Bratislava, Slovakia; [(b)]Department of Subnuclear Physics, Institute of Experimental Physics of the Slovak Academy of Sciences, Kosice, Slovak Republic
[30] Physics Department, Brookhaven National Laboratory, Upton, NY, USA
[31] Universidad de Buenos Aires, Facultad de Ciencias Exactas y Naturales, Departamento de Física, y CONICET, Instituto de Física de Buenos Aires (IFIBA), Buenos Aires, Argentina
[32] California State University, CA, USA
[33] Cavendish Laboratory, University of Cambridge, Cambridge, UK
[34] [(a)]Department of Physics, University of Cape Town, Cape Town, South Africa; [(b)]iThemba Labs, Western Cape, South Africa; [(c)]Department of Mechanical Engineering Science, University of Johannesburg, Johannesburg , South Africa; [(d)]National Institute of Physics, University of the Philippines Diliman (Philippines), Quezon City , Philippines; [(e)]Department of Physics, Stellenbosch University, Matieland, South Africa; [(f)]University of KwaZulu-Natal, School of Agriculture and Science, Mathematics, Westville, South Africa; [(g)]University of South Africa, Department of Physics, Pretoria, South Africa; [(h)]Department of Mechanical and Aeronautical Engineering, University of Pretoria, Pretoria, South Africa; [(i)]University of Zululand, KwaDlangezwa, South Africa; [(j)]School of Physics, University of the Witwatersrand, Johannesburg, South Africa
[35] Department of Physics, Carleton University, Ottawa, ON, Canada
[36] [(a)]Faculté des Sciences Ain Chock, Université Hassan II de Casablanca, Casablanca, Morocco; [(b)]Faculté des Sciences, Université Ibn-Tofail, Kénitra, Morocco; [(c)]Faculté des Sciences Semlalia, Université Cadi Ayyad, LPHEA-Marrakech, Marrakech, Morocco; [(d)]LPMR, Faculté des Sciences, Université Mohamed Premier, Oujda, Morocco; [(e)]Faculté des sciences, Université Mohammed V, Rabat, Morocco; [(f)]Institute of Applied Physics, Mohammed VI Polytechnic University, Ben Guerir, Morocco
[37] CERN, Geneva, Switzerland
[38] Affiliated with an Institute Formerly Covered by a Cooperation Agreement with CERN, Geneva, Switzerland
[39] Affiliated with an International Laboratory Covered by a Cooperation Agreement with CERN, Geneva, Switzerland

[40] Enrico Fermi Institute, University of Chicago, Chicago, IL, USA
[41] LPC, Université Clermont Auvergne, CNRS/IN2P3, Clermont-Ferrand, France
[42] Nevis Laboratory, Columbia University, Irvington, NY, USA
[43] Niels Bohr Institute, University of Copenhagen, Copenhagen, Denmark
[44] [(a)]Dipartimento di Fisica, Università della Calabria, Rende, Italy; [(b)]INFN Gruppo Collegato di Cosenza, Laboratori Nazionali di Frascati, Frascati, Italy
[45] Physics Department, Southern Methodist University, Dallas, TX, USA
[46] National Centre for Scientific Research "Demokritos", Agia Paraskevi, Greece
[47] [(a)]Department of Physics, Stockholm University, Stockholm, Sweden; [(b)]Oskar Klein Centre, Stockholm, Sweden
[48] Deutsches Elektronen-Synchrotron DESY, Hamburg and Zeuthen, Germany
[49] Fakultät Physik, Technische Universität Dortmund, Dortmund, Germany
[50] Institut für Kern- und Teilchenphysik, Technische Universität Dresden, Dresden, Germany
[51] Department of Physics, Duke University, Durham, NC, USA
[52] SUPA-School of Physics and Astronomy, University of Edinburgh, Edinburgh, UK
[53] INFN e Laboratori Nazionali di Frascati, Frascati, Italy
[54] Physikalisches Institut, Albert-Ludwigs-Universität Freiburg, Freiburg, Germany
[55] II. Physikalisches Institut, Georg-August-Universität Göttingen, Göttingen, Germany
[56] Département de Physique Nucléaire et Corpusculaire, Université de Genève, Geneva, Switzerland
[57] [(a)]Dipartimento di Fisica, Università di Genova, Genoa, Italy; [(b)]INFN Sezione di Genova, Genoa, Italy
[58] II. Physikalisches Institut, Justus-Liebig-Universität Giessen, Giessen, Germany
[59] SUPA-School of Physics and Astronomy, University of Glasgow, Glasgow, UK
[60] LPSC, Université Grenoble Alpes, CNRS/IN2P3, Grenoble INP, Grenoble, France
[61] Laboratory for Particle Physics and Cosmology, Harvard University, Cambridge, MA, USA
[62] Department of Modern Physics and State Key Laboratory of Particle Detection and Electronics, University of Science and Technology of China, Hefei, China
[63] [(a)]Kirchhoff-Institut für Physik, Ruprecht-Karls-Universität Heidelberg, Heidelberg, Germany; [(b)]Physikalisches Institut, Ruprecht-Karls-Universität Heidelberg, Heidelberg, Germany
[64] [(a)]Department of Physics, Chinese University of Hong Kong, Shatin, N.T., Hong Kong; [(b)]Department of Physics, University of Hong Kong, Hong Kong, China; [(c)]Department of Physics and Institute for Advanced Study, Hong Kong University of Science and Technology, Clear Water Bay, Kowloon, Hong Kong, China
[65] Department of Physics, National Tsing Hua University, Hsinchu, Taiwan
[66] IJCLab, Université Paris-Saclay, CNRS/IN2P3, 91405 Orsay, France
[67] Centro Nacional de Microelectrónica (IMB-CNM-CSIC), Barcelona, Spain
[68] Department of Physics, Indiana University, Bloomington, IN, USA
[69] [(a)]INFN Gruppo Collegato di Udine, Sezione di Trieste, Udine, Italy; [(b)]ICTP, Trieste, Italy; [(c)]Dipartimento Politecnico di Ingegneria e Architettura, Università di Udine, Udine, Italy
[70] [(a)]INFN Sezione di Lecce, Lecce, Italy; [(b)]Dipartimento di Matematica e Fisica, Università del Salento, Lecce, Italy
[71] [(a)]INFN Sezione di Milano, Milan, Italy; [(b)]Dipartimento di Fisica, Università di Milano, Milan, Italy
[72] [(a)]INFN Sezione di Napoli, Naples, Italy; [(b)]Dipartimento di Fisica, Università di Napoli, Naples, Italy
[73] [(a)]INFN Sezione di Pavia, Pavia, Italy; [(b)]Dipartimento di Fisica, Università di Pavia, Pavia, Italy
[74] [(a)]INFN Sezione di Pisa, Pisa, Italy; [(b)]Dipartimento di Fisica E. Fermi, Università di Pisa, Pisa, Italy
[75] [(a)]INFN Sezione di Roma, Rome, Italy; [(b)]Dipartimento di Fisica, Sapienza Università di Roma, Rome, Italy
[76] [(a)]INFN Sezione di Roma Tor Vergata, Rome, Italy; [(b)]Dipartimento di Fisica, Università di Roma Tor Vergata, Rome, Italy
[77] [(a)]INFN Sezione di Roma Tre, Rome, Italy; [(b)]Dipartimento di Matematica e Fisica, Università Roma Tre, Rome, Italy
[78] [(a)]INFN-TIFPA, Povo, Italy; [(b)]Università degli Studi di Trento, Trento, Italy
[79] Universität Innsbruck, Department of Astro and Particle Physics, Innsbruck, Austria
[80] Department of Physics and Astronomy, Iowa State University, Ames, IA, USA
[81] Istinye University, Sariyer, Istanbul, Türkiye
[82] [(a)]Departamento de Engenharia Elétrica, Universidade Federal de Juiz de Fora (UFJF), Juiz de Fora , Brazil; [(b)]Universidade Federal do Rio de Janeiro COPPE/EE/IF, Rio de Janeiro, Brazil; [(c)]Instituto de Física, Universidade de São Paulo, São Paulo, Brazil; [(d)]Rio de Janeiro State University, Rio de Janeiro , Brazil; [(e)]Federal University of Bahia, Bahia, Brazil

[83] KEK, High Energy Accelerator Research Organization, Tsukuba, Japan
[84] [(a)]Khalifa University of Science and Technology, Abu Dhabi, United Arab Emirates; [(b)]University of Sharjah, Sharjah, United Arab Emirates
[85] Graduate School of Science, Kobe University, Kobe, Japan
[86] [(a)]AGH University of Krakow, Faculty of Physics and Applied Computer Science, Kraków, Poland; [(b)]Marian Smoluchowski Institute of Physics, Jagiellonian University, Kraków, Poland
[87] Institute of Nuclear Physics Polish Academy of Sciences, Kraków, Poland
[88] Faculty of Science, Kyoto University, Kyoto, Japan
[89] Research Center for Advanced Particle Physics and Department of Physics, Kyushu University, Fukuoka, Japan
[90] L2IT, Université de Toulouse, CNRS/IN2P3, UPS, Toulouse, France
[91] Instituto de Física La Plata, Universidad Nacional de La Plata and CONICET, La Plata, Argentina
[92] Physics Department, Lancaster University, Lancaster, UK
[93] Oliver Lodge Laboratory, University of Liverpool, Liverpool, UK
[94] Department of Experimental Particle Physics, Jožef Stefan Institute and Department of Physics, University of Ljubljana, Ljubljana, Slovenia
[95] Department of Physics and Astronomy, Queen Mary University of London, London, UK
[96] Department of Physics, Royal Holloway University of London, Egham, UK
[97] Department of Physics and Astronomy, University College London, London, UK
[98] Louisiana Tech University, Ruston, LA, USA
[99] Fysiska institutionen, Lunds universitet, Lund, Sweden
[100] Departamento de Física Teorica C-15 and CIAFF, Universidad Autónoma de Madrid, Madrid, Spain
[101] Institut für Physik, Universität Mainz, Mainz, Germany
[102] School of Physics and Astronomy, University of Manchester, Manchester, UK
[103] CPPM, Aix-Marseille Université, CNRS/IN2P3, Marseille, France
[104] Department of Physics, University of Massachusetts, Amherst, MA, USA
[105] Department of Physics, McGill University, Montreal, QC, Canada
[106] School of Physics, University of Melbourne, Victoria, Australia
[107] Department of Physics, University of Michigan, Ann Arbor, MI, USA
[108] Department of Physics and Astronomy, Michigan State University, East Lansing, MI, USA
[109] Group of Particle Physics, University of Montreal, Montreal, QC, Canada
[110] Fakultät für Physik, Ludwig-Maximilians-Universität München, Munich, Germany
[111] Max-Planck-Institut für Physik (Werner-Heisenberg-Institut), Munich, Germany
[112] Graduate School of Science and Kobayashi-Maskawa Institute, Nagoya University, Nagoya, Japan
[113] [(a)]Department of Physics, Nanjing University, Nanjing, China; [(b)]School of Science, Shenzhen Campus of Sun Yat-sen University, Guangzhou, China; [(c)]University of Chinese Academy of Science (UCAS), Beijing, China
[114] Department of Physics and Astronomy, University of New Mexico, Albuquerque, NM, USA
[115] Institute for Mathematics, Astrophysics and Particle Physics, Radboud University/Nikhef, Nijmegen, Netherlands
[116] Nikhef National Institute for Subatomic Physics and University of Amsterdam, Amsterdam, Netherlands
[117] Department of Physics, Northern Illinois University, DeKalb, IL, USA
[118] [(a)]New York University Abu Dhabi, Abu Dhabi, United Arab Emirates; [(b)]United Arab Emirates University, Al Ain, United Arab Emirates
[119] Department of Physics, New York University, New York, NY, USA
[120] Ochanomizu University, Otsuka, Bunkyo-ku, Tokyo, Japan
[121] Ohio State University, Columbus, OH, USA
[122] Homer L. Dodge Department of Physics and Astronomy, University of Oklahoma, Norman, OK, USA
[123] Department of Physics, Oklahoma State University, Stillwater, OK, USA
[124] Palacký University, Joint Laboratory of Optics, Olomouc, Czech Republic
[125] Institute for Fundamental Science, University of Oregon, Eugene, OR, USA
[126] Graduate School of Science, University of Osaka, Osaka, Japan
[127] Department of Physics, University of Oslo, Oslo, Norway
[128] Department of Physics, Oxford University, Oxford, UK
[129] LPNHE, Sorbonne Université, Université Paris Cité, CNRS/IN2P3, Paris, France
[130] Department of Physics, University of Pennsylvania, Philadelphia, PA, USA

[131] Department of Physics and Astronomy, University of Pittsburgh, Pittsburgh, PA, USA
[132] [(a)]Laboratório de Instrumentação e Física Experimental de Partículas - LIP, Lisbon, Portugal; [(b)]Departamento de Física, Faculdade de Ciências, Universidade de Lisboa, Lisbon, Portugal; [(c)]Departamento de Física, Universidade de Coimbra, Coimbra, Portugal; [(d)]Centro de Física Nuclear da Universidade de Lisboa, Lisbon, Portugal; [(e)]Departamento de Física, Escola de Ciências, Universidade do Minho, Braga, Portugal; [(f)]Departamento de Física Teórica y del Cosmos, Universidad de Granada, Granada, Spain; [(g)]Departamento de Física, Instituto Superior Técnico, Universidade de Lisboa, Lisbon, Portugal
[133] Institute of Physics of the Czech Academy of Sciences, Prague, Czech Republic
[134] Czech Technical University in Prague, Prague, Czech Republic
[135] Charles University, Faculty of Mathematics and Physics, Prague, Czech Republic
[136] Particle Physics Department, Rutherford Appleton Laboratory, Didcot, UK
[137] IRFU, CEA, Université Paris-Saclay, Gif-sur-Yvette, France
[138] Santa Cruz Institute for Particle Physics, University of California Santa Cruz, Santa Cruz, CA, USA
[139] [(a)]Departamento de Física, Pontificia Universidad Católica de Chile, Santiago, Chile; [(b)]Millennium Institute for Subatomic Physics at High Energy Frontier (SAPHIR), Santiago, Chile; [(c)]Instituto de Investigación Multidisciplinario en Ciencia y Tecnología y Departamento de Física Universidad de La Serena, La Serena, Chile; [(d)]Universidad Andres Bello, Department of Physics, Santiago, Chile; [(e)]Universidad San Sebastian, Recoleta, Concepción, Chile; [(f)]Instituto de Alta Investigación, Universidad de Tarapacá, Arica, Chile; [(g)]Departamento de Física, Universidad Técnica Federico Santa María, Valparaíso, Chile
[140] Department of Physics, Institute of Science, Tokyo, Japan
[141] Department of Physics, University of Washington, Seattle, WA, USA
[142] [(a)]Institute of Frontier and Interdisciplinary Science and Key Laboratory of Particle Physics and Particle Irradiation (MOE), Shandong University, Qingdao, China; [(b)]School of Physics, Zhengzhou University, Zhengzhou, China
[143] [(a)]State Key Laboratory of Dark Matter Physics, School of Physics and Astronomy, Shanghai Jiao Tong University, Key Laboratory for Particle Astrophysics and Cosmology (MOE), SKLPPC, Shanghai, China; [(b)]State Key Laboratory of Dark Matter Physics, Tsung-Dao Lee Institute, Shanghai Jiao Tong University, Shanghai, China
[144] Department of Physics and Astronomy, University of Sheffield, Sheffield, UK
[145] Department of Physics, Shinshu University, Nagano, Japan
[146] Department Physik, Universität Siegen, Siegen, Germany
[147] Department of Physics, Simon Fraser University, Burnaby, BC, Canada
[148] SLAC National Accelerator Laboratory, Stanford, CA, USA
[149] Department of Physics, Royal Institute of Technology, Stockholm, Sweden
[150] Departments of Physics and Astronomy, Stony Brook University, Stony Brook, NY, USA
[151] Department of Physics and Astronomy, University of Sussex, Brighton, UK
[152] School of Physics, University of Sydney, Sydney, Australia
[153] Institute of Physics, Academia Sinica, Taipei, Taiwan
[154] [(a)]E. Andronikashvili Institute of Physics, Iv. Javakhishvili Tbilisi State University, Tbilisi, Georgia; [(b)]High Energy Physics Institute, Tbilisi State University, Tbilisi, Georgia; [(c)]University of Georgia, Tbilisi, Georgia
[155] Department of Physics, Technion, Israel Institute of Technology, Haifa, Israel
[156] Raymond and Beverly Sackler School of Physics and Astronomy, Tel Aviv University, Tel Aviv, Israel
[157] Department of Physics, Aristotle University of Thessaloniki, Thessaloniki, Greece
[158] International Center for Elementary Particle Physics and Department of Physics, University of Tokyo, Tokyo, Japan
[159] Graduate School of Science and Technology, Tokyo Metropolitan University, Tokyo, Japan
[160] Department of Physics, University of Toronto, Toronto, ON, Canada
[161] [(a)]TRIUMF, Vancouver, BC, Canada; [(b)]Department of Physics and Astronomy, York University, Toronto, ON, Canada
[162] Division of Physics and Tomonaga Center for the History of the Universe, Faculty of Pure and Applied Sciences, University of Tsukuba, Tsukuba, Japan
[163] Department of Physics and Astronomy, Tufts University, Medford, MA, USA
[164] Department of Physics and Astronomy, University of California Irvine, Irvine, CA, USA
[165] University of West Attica, Athens, Greece
[166] Department of Physics and Astronomy, University of Uppsala, Uppsala, Sweden
[167] Department of Physics, University of Illinois, Urbana, IL, USA
[168] Instituto de Física Corpuscular (IFIC), Centro Mixto Universidad de Valencia - CSIC, Valencia, Spain

[169] Department of Physics, University of British Columbia, Vancouver, BC, Canada
[170] Department of Physics and Astronomy, University of Victoria, Victoria, BC, Canada
[171] Fakultät für Physik und Astronomie, Julius-Maximilians-Universität Würzburg, Würzburg, Germany
[172] Department of Physics, University of Warwick, Coventry, UK
[173] Waseda University, Tokyo, Japan
[174] Department of Particle Physics and Astrophysics, Weizmann Institute of Science, Rehovot, Israel
[175] Department of Physics, University of Wisconsin, Madison, WI, USA
[176] Fakultät für Mathematik und Naturwissenschaften, Fachgruppe Physik, Bergische Universität Wuppertal, Wuppertal, Germany
[177] Department of Physics, Yale University, New Haven, CT, USA
[178] Yerevan Physics Institute, Yerevan, Armenia

[a] Also at Affiliated with an Institute Formerly Covered by a Cooperation Agreement with CERN, Geneva, Switzerland
[b] Also at An-Najah National University, Nablus, Palestine
[c] Also at Borough of Manhattan Community College, City University of New York, New York, NY, USA
[d] Also at Center for Interdisciplinary Research and Innovation (CIRI-AUTH), Thessaloniki, Greece
[e] Also at Centre of Physics of the Universities of Minho and Porto (CF-UM-UP), Porto, Portugal
[f] Also at CERN, Geneva, Switzerland
[g] Also at Département de Physique Nucléaire et Corpusculaire, Université de Genève, Genève, Switzerland
[h] Also at Departament de Fisica de la Universitat Autonoma de Barcelona, Barcelona, Spain
[i] Also at Department of Financial and Management Engineering, University of the Aegean, Chios, Greece
[j] Also at Department of Mathematical Sciences, University of South Africa, Johannesburg, South Africa
[k] Also at Department of Modern Physics and State Key Laboratory of Particle Detection and Electronics, University of Science and Technology of China, Hefei, China
[l] Also at Department of Physics, Bolu Abant Izzet Baysal University, Bolu, Türkiye
[m] Also at Department of Physics, King's College London, London, UK
[n] Also at Department of Physics, Stanford University, Stanford, CA, USA
[o] Also at Department of Physics, Stellenbosch University, South Africa
[p] Also at Department of Physics, University of Fribourg, Fribourg, Switzerland
[q] Also at Department of Physics, University of Thessaly, Greece
[r] Also at Department of Physics, Westmont College, Santa Barbara, USA
[s] Also at Faculty of Physics, Sofia University, 'St. Kliment Ohridski', Sofia, Bulgaria
[t] Also at Faculty of Physics, University of Bucharest, Romania
[u] Also at Hellenic Open University, Patras, Greece
[v] Also at Henan University, Kaifeng, China
[w] Also at Imam Mohammad Ibn Saud Islamic University, Riyadh, Saudi Arabia
[x] Also at Institucio Catalana de Recerca i Estudis Avancats, ICREA, Barcelona, Spain
[y] Also at Institut für Experimentalphysik, Universität Hamburg, Hamburg, Germany
[z] Also at Institute for Nuclear Research and Nuclear Energy (INRNE) of the Bulgarian Academy of Sciences, Sofia, Bulgaria
[aa] Also at Institute of Applied Physics, Mohammed VI Polytechnic University, Ben Guerir, Morocco
[ab] Also at Institute of Particle Physics (IPP), Victoria, Canada
[ac] Also at Institute of Physics and Technology, Mongolian Academy of Sciences, Ulaanbaatar, Mongolia
[ad] Also at Institute of Physics, Azerbaijan Academy of Sciences, Baku, Azerbaijan
[ae] Also at Institute of Theoretical Physics, Ilia State University, Tbilisi, Georgia
[af] Also at Millennium Institute for Subatomic physics at high energy frontier (SAPHIR), Santiago, Chile
[ag] Also at National Institute of Physics, University of the Philippines Diliman (Philippines), Philippines
[ah] Also at The Collaborative Innovation Center of Quantum Matter (CICQM), Beijing, China
[ai] Also at TRIUMF, Vancouver, BC, Canada
[aj] Also at Università di Napoli Parthenope, Naples, Italy
[ak] Also at University of Chinese Academy of Sciences (UCAS), Beijing, China
[al] Also at Department of Physics, University of Colorado Boulder, Boulder, CO, USA
[am] Also at University of Siena, Siena, Italy

[an] Also at Washington College, Chestertown, MD, USA
[ao] Also at Yeditepe University, Physics Department, Istanbul, Türkiye
* Deceased